Project Number: DJO-0307

Department of Mechanical Engineering

BLEED FLOW EFFECTS ON INGESTED HAIL PARTICLES

A Major Qualifying Project Report:

Submitted to the Faculty

of the

WORCESTER POLYTECHNIC INSTITUTE

in partial fulfillment of the requirements for the

Degree of Bachelor of Science

by

Shaun Comee

Gregor Kevrekian

Sarah Taylor

March 1, 2007

Professor David J. Olinger, Advisor

Abstract

The station 2.5 bleed in Pratt & Whitney turbofan engines is designed to ingest hail particles as they pass through the engine. This keeps ice from entering the combustor and causing a possible engine flameout. To determine if the station 2.5 bleed is performing up to FAA standards, Pratt & Whitney conducts hail ingestion tests on a rig instead of full engines.

The purpose of this MQP is to assist Pratt & Whitney in more precisely determining sensitivity of certain rig parameters to allow more optimal setting of those parameters within the rig. Fluent software was used to compute the flow fields in the immediate vicinity of the station 2.5 bleed for both engine and rig cases. A Matlab code was written to numerically simulate the predicted trajectory of hail particles as they pass through the flow fields of the engine and rig. The predicted trajectory deflections of ice particles passing through both the engine and rig were compared order to better understand the test sensitivity to the inlet flow differences.

Results indicate that particle deflections in the rig approximately match those experienced by particles traveling though the engine across a wide range of input parameters such as particle diameter, initial velocity and initial position. However, for particles smaller than .02in in diameter deflections in the rig are as much as an order of magnitude greater than those seen in the engine.

Results also indicate that ballistic effects play a much stronger role in determining particle trajectory than aerodynamic effects for average ice particle sizes. Average hail particle diameter is 0.05 inches. Typical aerodynamically induced particle deflections were on the order of 1/100 inches in both engine and rig for average sized ice particles.

Table of Contents

Table of Figures

Table of Tables

Acknowledgments

Special thanks to Justin Urban and Kyle Vander Poel of Pratt & Whitney and our project advisor Professor David J. Olinger of the Worcester Polytechnic Institute.

Introduction

The goal of this project is to more precisely determine the sensitivity of certain parameters for the rig that Pratt & Whitney utilizes to satisfy hail ingestion testing that is required by the Federal Aviation Administration (FAA). The FAA requires that all aircraft engine manufacturers test their engines against a simulated "one-in-a-billion" hailstorm.

The rig that Pratt & Whitney uses draws air in via vacuum downstream of the station 2.5 bleed inlet rather than "ramming" air in through the engine inlet. Pratt & Whitney is interested in improving the understanding of the flow field near the bleed inlet in the rig and the manner in which this flow field changes the trajectory of ice particles that are injected into the flow. They are also interested in comparing the influence of the bleed flow on the particles in the rig versus the influence on the particles in the engine.

The first step to completing this project was the creation of a two-dimensional virtual model for both the rig and engine. This was accomplished using the software Gambit. Gambit is the geometry and mesh generation software included with the CFD analysis software, Fluent. Gambit's single interface for geometry creation and meshing brings together most of Fluent's preprocessing technologies in one environment.

After constructing these models, Fluent was used to complete a computational fluid dynamics analysis. Fluent is a general purpose CFD software package whose software code is based on the finite volume method on a collocated grid. Fluent incorporates dynamic meshing that can efficiently handle the type of fluid flow studied in this project. Fluent solved for the flow fields from which valuable information could be extracted such as air velocity throughout the bleed.

In order to determine the trajectory of ice particles, a code was constructed using Matlab version 2006a. This code uses the flow field data generated in Fluent (nodal positions and x,y

components of velocity) to determine how a ice particle's trajectory will be influenced by the flow field. The user has the option to change various input parameters of the code in order to allow flexibility in testing and data acquisition. The data gathered using the MatLab code was analyzed in order to determine the capacity of the rig in recreating the conditions seen in the engine during flight.

Background

Numbered stations identify locations within an aircraft engine. Station one is the inlet, station two is the entry to the low-pressure compressor, station three is the exit of the high-pressure compressor, station four marks the exit of the combustion chamber and the rest of the stations in the engine are marked by increasing numbers as they approach the exhaust nozzle. These components can be seen below in Figure 1.

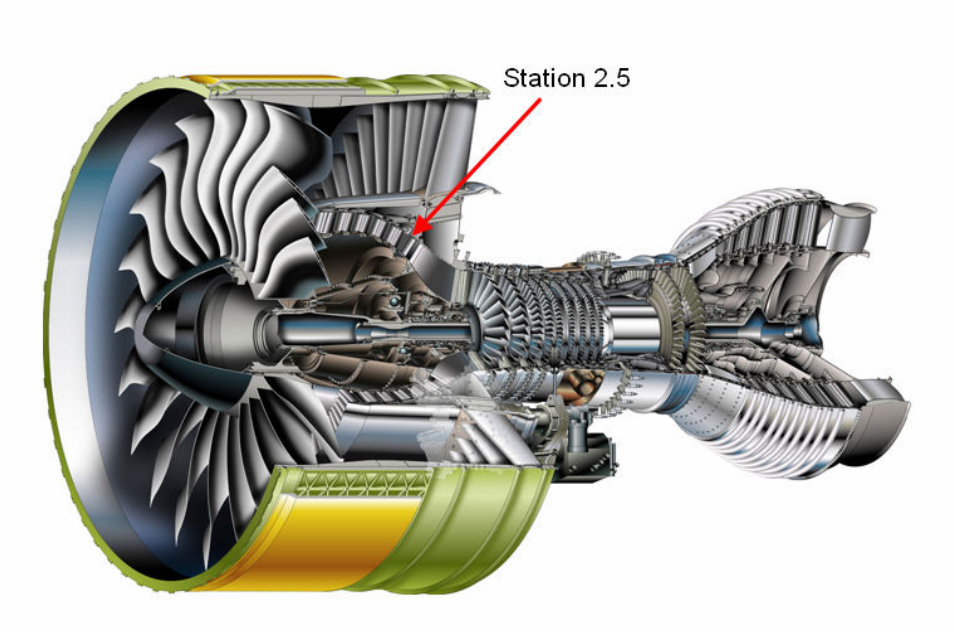

Figure 1: GP7000 engine with station 2.5 labeled

Within the engine, there are several bleeds which serve a variety of functions. Some typical functions of an air bleed are venting of high pressures to prevent engine stalls, redirecting heated air into passenger areas or for use to prevent ice formation on critical aircraft components.

Of particular interest to this project is the station 2.5 bleed which can be seen in Figure 2. The ".5" indicates that it is located in the center of the compressor, between the low pressure and high-pressure compressor. This bleed serves two main purposes. At lower power settings, the low-pressure compressor (LPC) is more efficient than the high-pressure compressor (HPC), so

the LPC delivers more compressed air than the HPC can accept. This would lead to a buildup of pressure at station 2.5, creating a back pressure that would cause the LPC airfoil blades to stall. The 2.5 bleed is there to open at low power settings (< 80% engine speed) and alleviate this pressure. The second purpose, and the one of interest to this project, is to rid the engine of ice and water during hail and rainstorms.

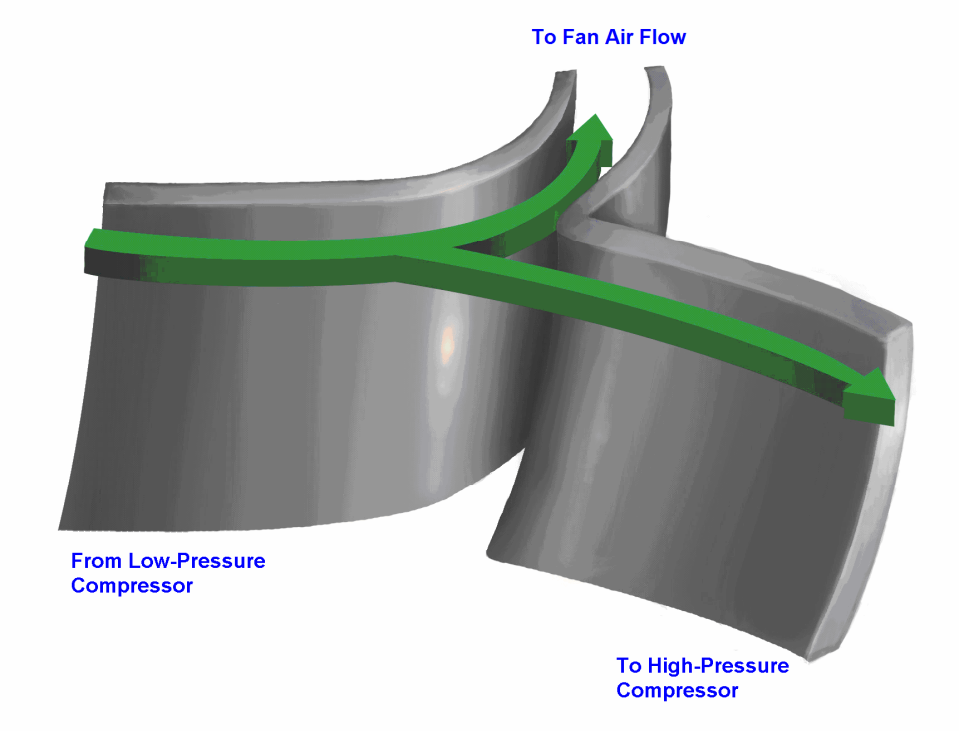

Figure 2: Station 2.5 bleed

The 2.5 bleed is a slot in the outer wall of the flow channel in the engine. It can be opened or closed (usually it is open at low speeds when extra air from the LPC must be dumped overboard) by the engine's computer, called the Full Authority Digital Electronics Control or FADEC. In normal operation the FADEC automatically determines when to open the bleeds based on sensor readings of pressure, rpm, temperature, and other variables. This bleed leads into a divergent duct that pulls some of the air out of the main flow channel. The air is then expelled out of the engine, into the bypass flow behind the large inlet fan[1].

FAA Hail Test Requirements

Hail ingestion testing is mandated by the FAA due to the severity of problems hail can cause to an engine in flight. Hail can cause damage to fan blades or other components of the engine and in the worst of cases may cause the engine to flameout as melted hail enters the combustion chamber, removing thermal energy.

There are several reported cases of multiple engine flameouts caused by flying into a hailstorm, however catastrophes are generally avoidable since the pilot can attempt to restart any engines that have ceased to operate. Engine flameout is particularly dangerous during landing descent because the engine power setting is low and the engine has the lowest tolerance against hail. Recovery is difficult or even impossible in during this phase of flight. The altitude at which a descending aircraft must fly and the typical altitude at which the hail-to-air ratio is highest is between 5,000 and 20,000 feet[3].

Rain, snow, and hail must be removed from the airflow entering an engine in order to avoid flameout. The station 2.5 engine bleed is designed so that the ill-effects caused by flying through a hailstorm are usually negated. A typical hailstorm does not result in enough water accumulation in the engine to pose a large danger to today's engines. High temperatures in the combustor evaporate a large amount of the moisture generated from the melted hail. The steam in the fuel-air mixture produced by this evaporated hail accounts for only a small loss of power in the engine unless the amount of water vapor introduced into the mixture is large. The engine is designed to remove excessive water and hail from the main flow path and guide it to the bypass flow. Since this flow does not pass through the combustor, power loss is avoided[2].

According to FAA documentation[3] the FAA requires in its test that "the ingestion of large hailstones (0.8 to 0.9 specific gravity) at the maximum true air speed, up to 15,000 feet, associated with a representative aircraft operating in rough air, with the engine at maximum

continuous power, may not cause unacceptable mechanical damage or unacceptable power or thrust loss after the ingestion, or require the engine to be shut down." [3]

In order to simulate a hailstorm in an engine, one-half of the required number of hailstones are aimed randomly over the inlet face area and the other half are aimed at the critical inlet face area. The critical inlet face area is defined as the portion of the inlet that leads directly toward the core of the engine rather than through the bypass. The hailstones must be ingested in a rapid sequence to simulate a hailstone encounter and the number and size of the hailstones are determined as follows:

- One 1-inch diameter hailstone for engines with inlet areas of not more than 100 square inches.[3]
- One 1-inch diameter hailstone and one 2-inch diameter hailstone for each 150 square inches of inlet area, or fraction thereof, for engines with inlet areas of more than 100 square inches.[3]

It must be shown that each engine is capable of acceptable operation through its specified operating envelope when subjected to sudden encounters with the certification standard concentrations of hail as detailed in Tables 1 and 2 below. Acceptable engine operation precludes flameout, run down, continued or non-recoverable surge or stall, or loss of acceleration and deceleration capability, during any 30 second continuous period in hail. There must also be no unacceptable power or thrust loss or other adverse engine anomalies following the ingestion.[3]

In conducting tests, hail fabricated from ice must be delivered to the engine having the shapes, sizes and distributions of sizes of those defined in the following tables. Alternatively, the use of a single size or shape for each hailstone can be accepted provided that the engine manufacturer shows that the substitution does not reduce the severity of the test[4].

Table 1: Certification Standard Atmospheric Hail Concentrations

Altitude (feet)	Hail Water Content (HWC) (grams water/cubic meter air)
0	6.0
7300	8.9
8500	9.4
10000	9.9
12000	10.0
15000	10.0
16000	8.9
17700	7.8
19300	6.6
21500	5.6
24300	4.4
29000	3.3
46000	0.2

Table 2: Certification Standard Atmospheric Hail Size Distribution

Hail Diameter (mm)	Contribution to total hail water content (HWC) (%)
0 - 4.9	0.00
5.0 - 9.9	17.00
10.0 - 14.9	25.00
15.0 - 19.9	22.50
20.0 - 24.9	16.00
25.0 - 29.9	9.75
30.0 - 34.9	4.75
35.0 - 39.9	2.50
40.0 - 44.9	1.50
45.0 - 49.9	0.75
50.0 - 55.0	0.25

The rig that Pratt & Whitney uses differs from the rigs that other aircraft engine manufacturers use in that a full engine is not used in the test. Under normal hail ingestion test circumstances, hail is propelled at the entire inlet area of a full engine while in operation. Conceptually, if the engine successfully completes the test without an occurrence of one of the unacceptable engine problems as specified by the FAA, then the engine passes. Pratt & Whitney on the other hand, uses a combination of analysis and component rig testing to satisfy the requirement. One particular rig tests confirms the capability of the station 2.5 bleed, which is

being studied in this project. The thermodynamic and physical properties of incoming air flow at the 2.5 bleed are known based on the results of a flow simulation and engine tests run by Pratt & Whitney.

A 45-degree section of the annulus is used as a representative section. With an engine in flight, the incoming air has a swirl component and approximately 10% of the oncoming gas path flow is able to feed the entire bleed inlet. In the rig, there is only a 45-degree arc of the annulus, the flow is not swirling, and the air is being drawn in via a vacuum downstream of the bleed inlet rather than being rammed in and vacuumed as in in-flight conditions[5].

In this project, the bleed influence on the hail particles in the rig are to be compared to the bleed influence on the particles in the engine. It is believed by some at Pratt & Whitney that the rig is an invalid simulation of a real engine and that a real engine ingests more ice particles than the test rig. Others believe that the test rig in fact, ingests more ice particles than the engine.

Summary

Problem Statement

Pratt & Whitney uses a rig to perform FAA required hail ingestion certification. A 45-degree section of the full annulus of the station 2.5 bleed is used as a representative section to perform the test. In the engine, the flow upstream of the bleed has a swirl component to it and approximately 10% of the oncoming gas path flow is able to feed the entire bleed inlet. Within the rig, there is only 45 degrees of arc, the flow is not swirling, and the air is being drawn in via vacuum downstream of the bleed inlet instead of being "rammed" in and vacuumed like in the engine. Pratt & Whitney is interested in improving their understanding of how that flow field changes the trajectory of ice particles that are following a known trajectory until influenced by the bleed flow. In addition, a comparison was made between the bleed influence on the particles in the rig and the bleed influence on the particles in the engine.

Project Goals

1. Develop and run two-dimensional computational fluid dynamics (CFD) simulations of the station 2.5 bleed modeling Pratt & Whitney's hail ingestion certification rig.
2. Develop and run two-dimensional computational fluid dynamics (CFD) simulations of the station 2.5 bleed modeling the actual engine.
3. Determine the trajectory of a hail particle as it attempts to pass by the bleed inlet in the rig and compare it to the trajectory as seen in the engine model.

Methodology

The Bleed Geometry

The first step in finding the trajectory of a hail particle in the station 2.5 engine bleed was to digitize the geometry of the 2.5 bleed. The information provided about the bleed geometry was in the form of a hard copy sketch which is shown in Figure 3 below.

The liaisons at Pratt and Whitney supplied a LabView program referred to as the "graph decomposer." To use the program, the picture of the bleed inlet was scanned into a computer, imported into Microsoft PowerPoint and copied into the graph decomposer main window. The outline of the bleed was then traced while the program, utilizing a "while loop" structure, recorded the position of the cursor. Using this program, the picture was digitized this into a set of Cartesian coordinate points representing the bleed. Data points were recorded for the entire bleed geometry and stagnation streamline, and stored in Microsoft Excel. Stagnation streamline data points were used in the engine model but not in the rig as will be explained later. The graph decomposer window can be seen in Figure 4 below.

The resulting bleed geometry data points extracted from LabView were in correct proportion to one another, however, the entire set of data points needed to be properly scaled to accurately represent the bleed dimensions. Using the known bleed-opening dimension of 1-inch and basic trigonometry equations, the necessary scaling factor of 2 was determined. With the data points accurately scaled, a complete set of points which exactly represented the bleed geometry was obtained.

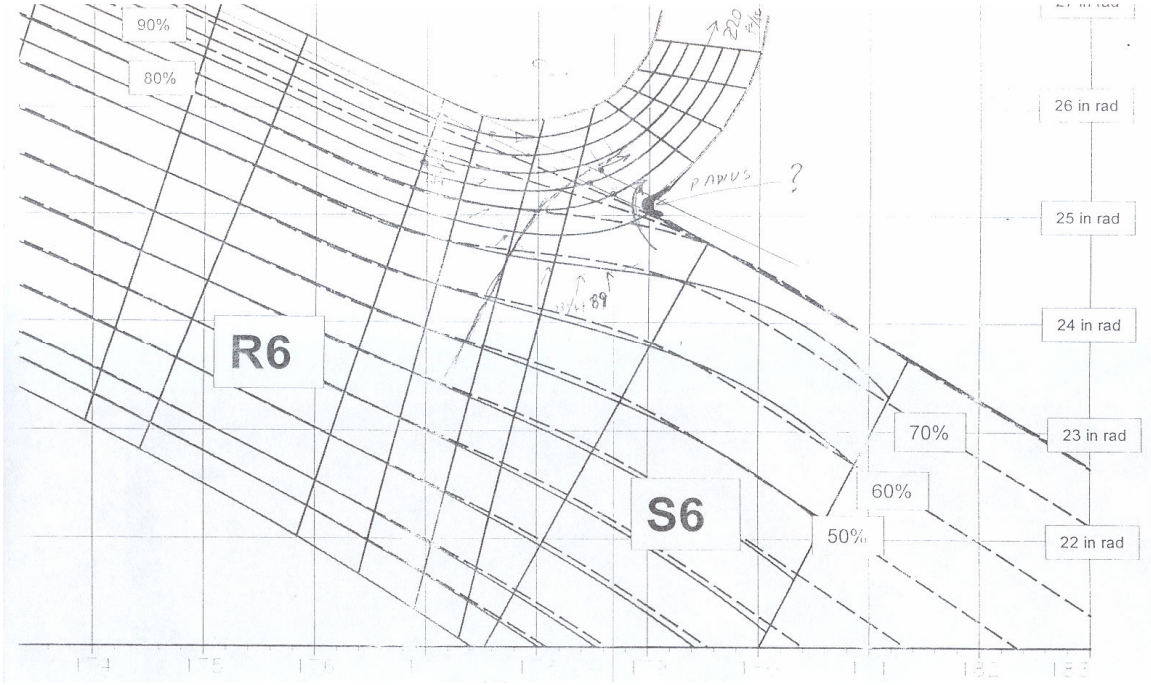

Figure 3: Station 2.5 bleed sketch with stagnation streamline

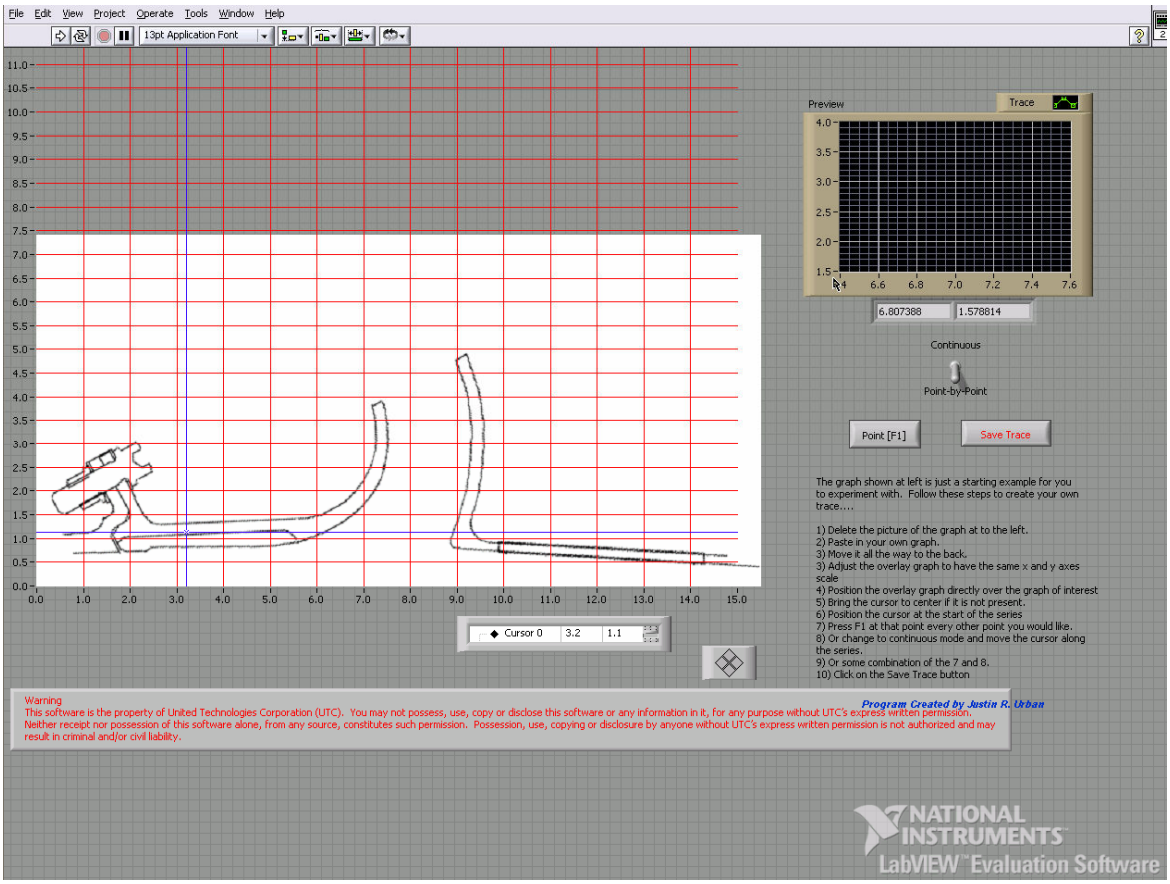

Figure 4: Graph decomposer interface

Meshing Geometry in Gambit

The Computational Fluid Dynamics (CFD) software used for this project was Fluent version 6.2.16. Fluent is set up to receive pre-constructed geometries for which the area of interest is already discretized into a mesh. Gambit is the program used for meshing and developed by the maker of Fluent.

To construct the rig bleed geometry in Gambit, each of the scaled data points were entered into the program by their Cartesian coordinates. All coordinates except for those of the stagnation streamline were used in constructing the rig model. All coordinates except for those to the right of the intersection of the stagnation streamline and right side of the bleed were used for the final version of the engine model. Lines were then constructed between the data points in Gambit, forming a 2D cross-sectional "slice" of the bleed. Bezier curves were inserted to create the best fitting lines through areas of smooth curvature.

In the rig, air is drawn through the bleed via vacuum whereas in the engine air is "rammed" into the bleed as the aircraft moves through the air. In order to accurately represent both scenarios, the engine model and rig model were constructed differently.

In the rig model, a semicircular boundary was used. The vacuum pulls air into the bleed equally from all directions around the base of the bleed, making a half-circle a good choice. Flow across this boundary is specified as perpendicular to the boundary.

Based on information provided by our liaison, a "stagnation streamline" is known to exist in the flow field for actual engine flow. All flow above the stagnation streamline will go into the bleed, and all flow below this streamline will not go into the bleed since velocity is tangential to a streamline (there can be no flow across the stagnation streamline). Consequently, in the engine

model, only flow above this streamline is considered. Any flow below this is of no concern and does not affect the hail particles entering the area above the streamline.

Initially, a model of different shape was constructed for the engine. This model was based off using the centerline of the engine as an "axis" boundary. This model can be seen in Figure 5. Upon completing this model, running it through the CFD analysis in Fluent, and presenting to our Pratt & Whitney liaisons, it was decided that the stagnation streamline would be a better boundary. First, the original model was much too large for what was needed. The centerline was 25 inches away from the bottom of the bleed and the flow field of interest lies only about an inch below the bleed inlet. Second, the stagnation streamline found in the original model looked nearly identical to the stagnation streamline in the bleed sketch provided earlier. It was decided that the model was accurate enough to remove the large area below this line and construct a new model that involved only the section between the top wall of the engine and the stagnation streamline. Figure 6 shows the streamline plot and the stagnation point is circled.

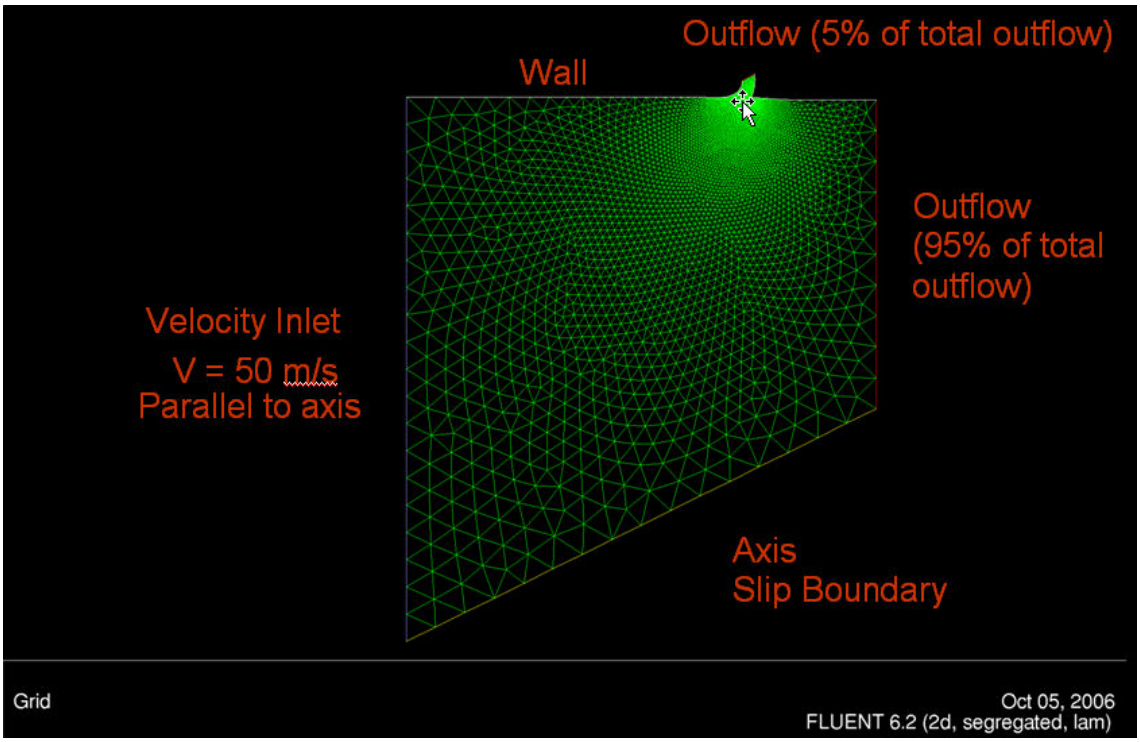

Figure 5: Original engine model using an axis slip boundary

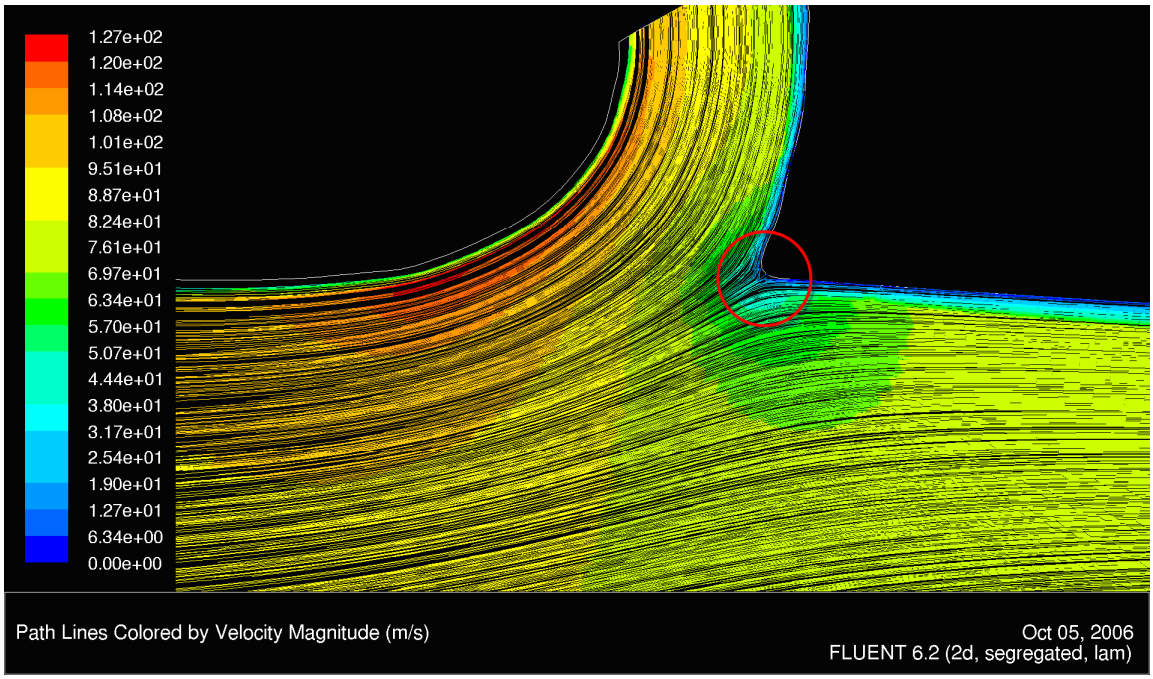

Figure 6: Original engine model streamline plot

Gambit requires each surface to be defined according to a particular boundary type. Essentially, the user must specify which surfaces are non-porous "walls" and which surfaces allow the passage of flow. When the mesh is exported from Gambit to Fluent, the exact conditions at each boundary are specified. This is the information the program needs generate a solution.

There are 22 ways to define a boundary in Gambit; some of these include wall, velocity inlet, and outflow. A compiled list of frequently used boundary types is shown in Appendix A.

In constructing the rig model, three boundary types were used. Solid walls with no-slip conditions were used for the top surface and sides of the bleed geometry which represents the surface of the aircraft engine. A mass flow rate inlet was specified for the half-circle boundary and an outflow boundary condition was used for the bleed exit. Mass flow rate inlet was the best choice for the half-circle boundary since this data was readily available and was a common parameter to both the engine and rig.

The mass flow rate was specified as 3.4087 lbm/s (1.546 kg/s). This number was found using the data provided by Pratt & Whitney which specified 1.7 lbm/s of flow through a 45° arc section of the test rig. Using the radius of the annulus, the mass flow rate per unit depth was calculated. Since Fluent assigns two-diensional models a depth of unity, the mass flow rate per unit depth was needed. Using mass flow rate avoided possible discrepancies between the rig and engine models caused by inconsistencies in boundary condition data.

The outflow boundary condition option is used to model exit flows where the details of the flow velocity and pressure are not known prior to solution of the flow problem. This is the case with this model, making it the best choice for this particular situation.

For the final engine model, the same boundary types were used with the addition of an axis boundary, similar to the one mentioned before in constructing the early engine model. The

top surface and sides of the bleed were defined as solid walls. The exit of the bleed was chosen to be an outflow, the left side of the model was the mass flow inlet, and the lower surface was defined as an axis. An axis allows for slip velocity, unlike a solid wall. This is required here since the lower surface is a stagnation streamline that was traced from the flow field sketch.

The conditions in the engine bleed were given by a computer simulation of the engine conditions at the 2.5 station. The program was run by the Propulsion Systems Analysis department at Pratt & Whitney. The conditions included temperature, Mach number, and pressure. Density was found using the ideal gas law.

The final step in completing the rig and engine models was to create a mesh. Mesh resolution is of great importance to the accuracy of any CFD solution. Essentially, the solution accuracy increases with decreasing cell size. There is however a threshold to the improvement in accuracy. Beyond this threshold, making the mesh finer increases solution run-time without any appreciable gain in accuracy. Several meshes were generated for both the rig and engine model to find the accuracy threshold, where the resultant flow field was independent of the grid resolution.

It is also worth noting that the grid resolution dictates the number of available data points which are used in the particle trajectory prediction code, described later. Though it would be possible to find accurate flow information from larger celled grids than were used, more cells provide more detailed information for the particle trajectory program in MatLab. The grids were coarse enough to run quickly so optimization was less of an issue than providing enough data for the trajectory program. The grids were made finest in the areas of interest and coarser in other areas. The final rig and engine models can be seen in Figures 7 and 8 respectively, with boundary types specified and models completely meshed.

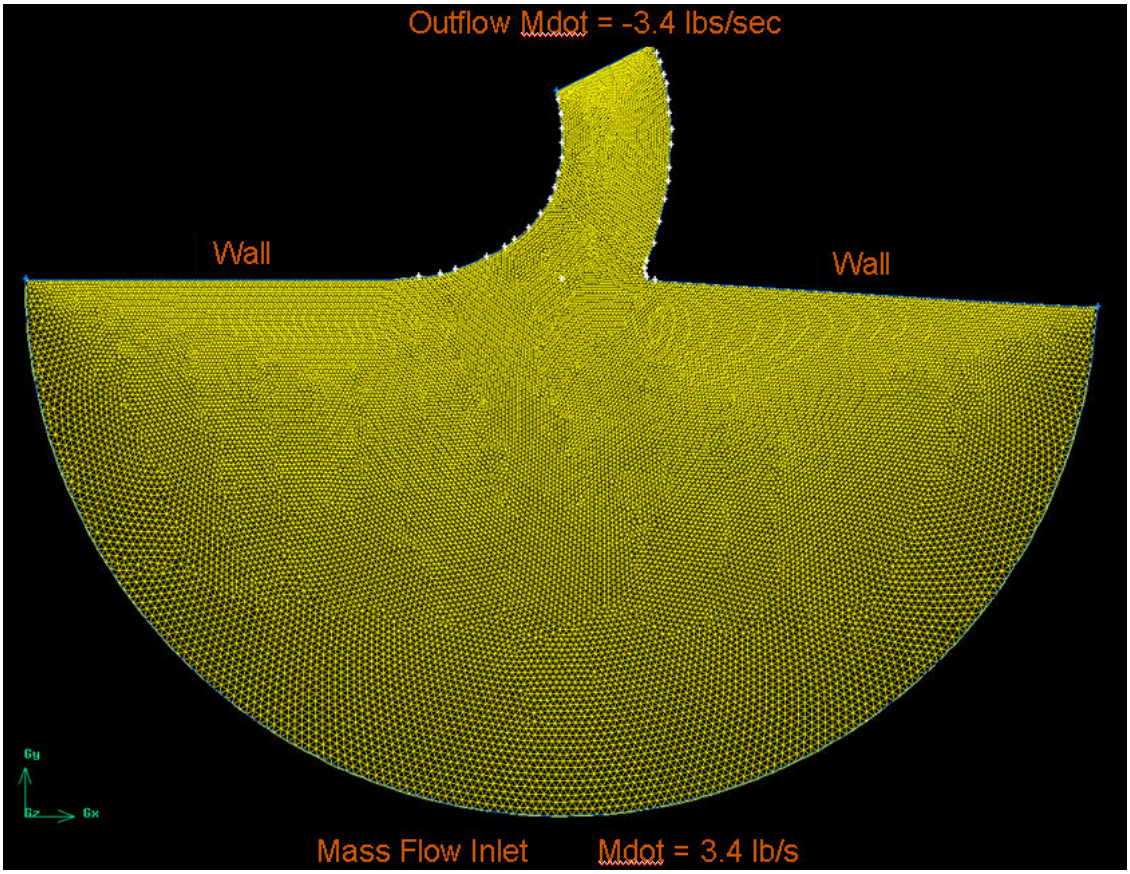

Figure 7: Final rig model showing meshing and boundary types

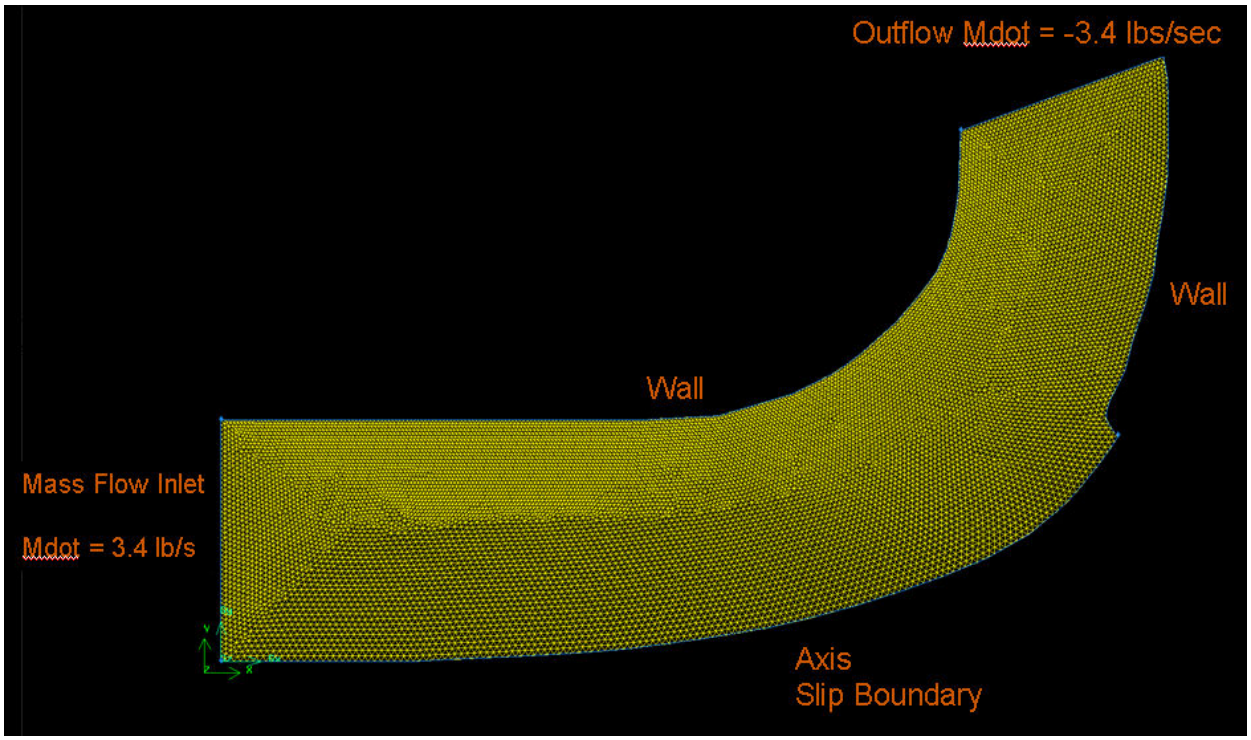

Figure 8: Final engine model showing meshing and boundary types

Fluent Code

The next step was to export the mesh from Gambit into Fluent. Of primary importance in Fluent is the specification of the boundary conditions (BC). Fluent provides multiple options which the user can specify relating to the operating conditions, solver type, and simplifications. In general, simplifying assumptions (i.e. ideal gas, convergence criterion, etc.) will tend to decrease both run-time and the possibility of divergent solutions. However, over simplification can also decrease accuracy of the solution. As the skills of this group with respect to Fluent grew, the complexity of the models also grew by eliminating assumptions whenever possible. The exact input parameters used can be seen in Appendix B.

Flow field solutions for the engine and rig can be seen below in Figures 9 through 16. Figures 9 and 10 show the velocity magnitude contour plots for the rig and engine. It is clearly seen that the flow in the rig starts from a very small velocity and accelerates into the bleed due to the vacuum. Flow around the inside edge of the bleed is accelerated to a greater speed than the right side due to the shape of the bleed. In the engine model, the same results are found however the fluid is entering with an initial velocity rather than starting at zero velocity.

Figures 15 and 16 show the static pressure contour plots. These follow the Bernoulli effect in that pressure is highest where there is lowest velocity. The near-zero velocity region in the rig model has the highest pressure and the lowest pressure occurs around the inside bend of the bleed. An important point to notice is in Figure 16 near the end of the stagnation streamline boundary. A stagnation streamline ends in a stagnation point and it can be clearly seen from this figure that the pressure surrounding that particular corner is the highest pressure in the model.

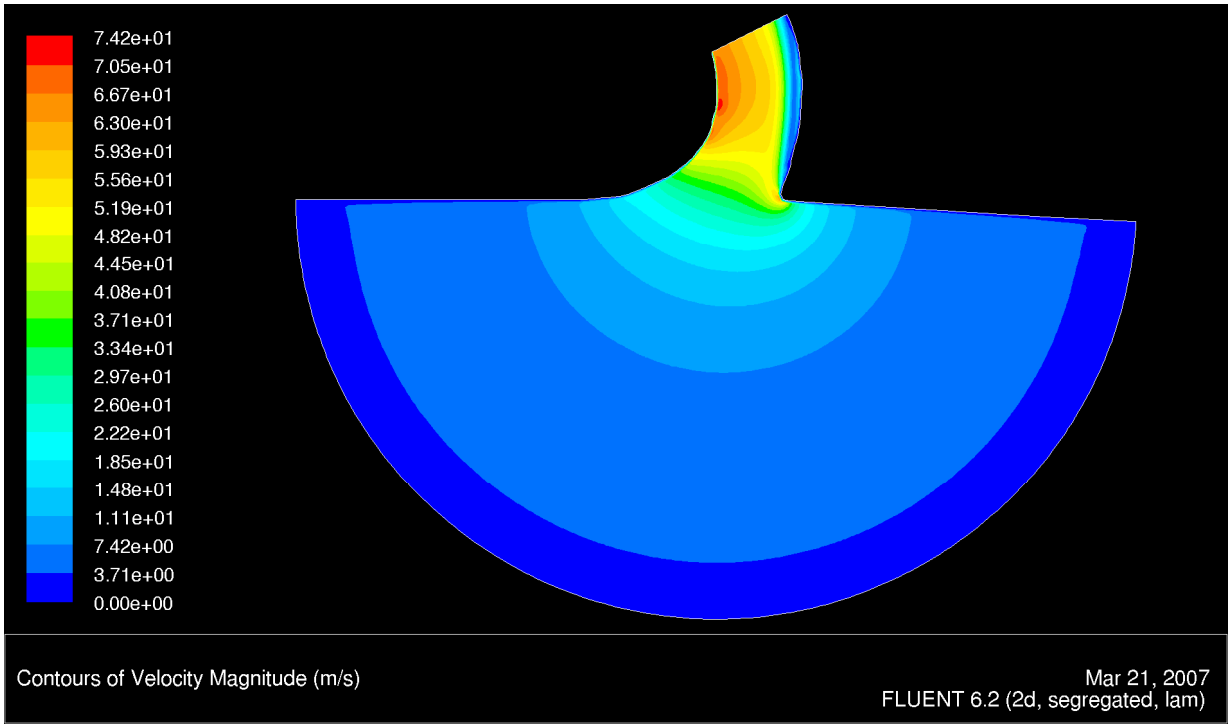

Figure 9: Rig model - velocity contour plot

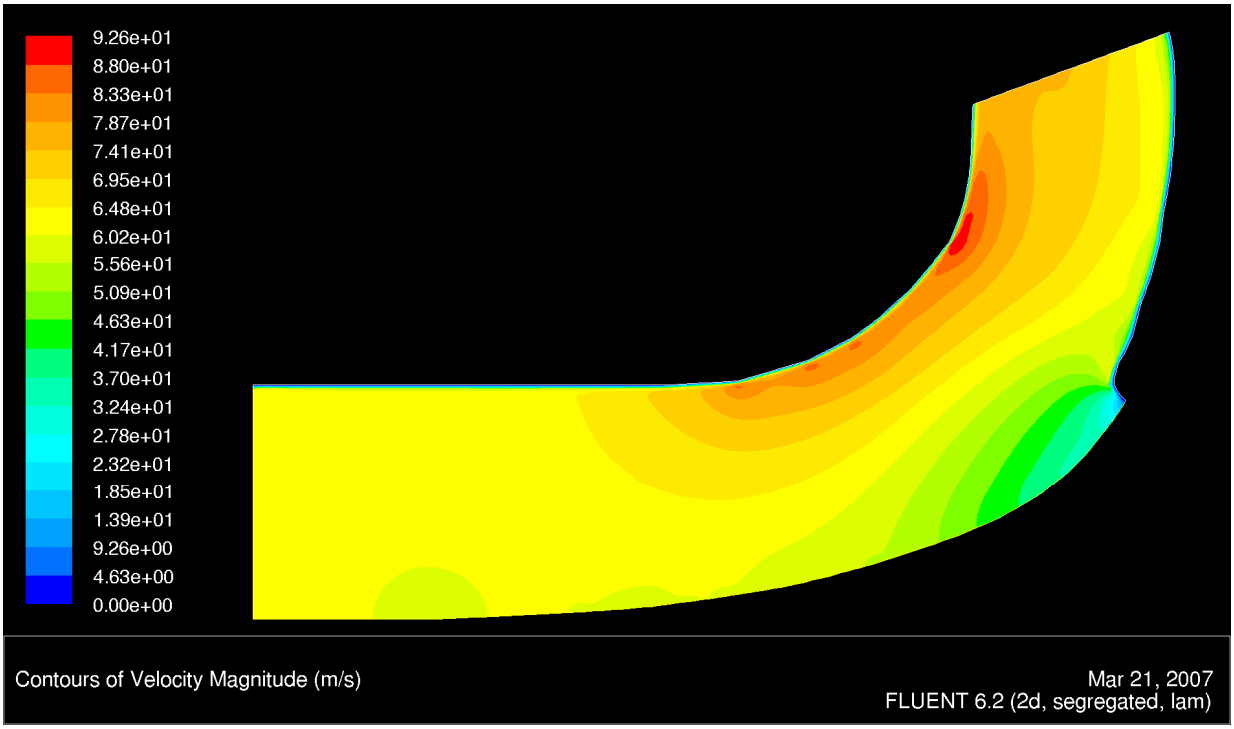

Figure 10: Engine model - velocity contour plot

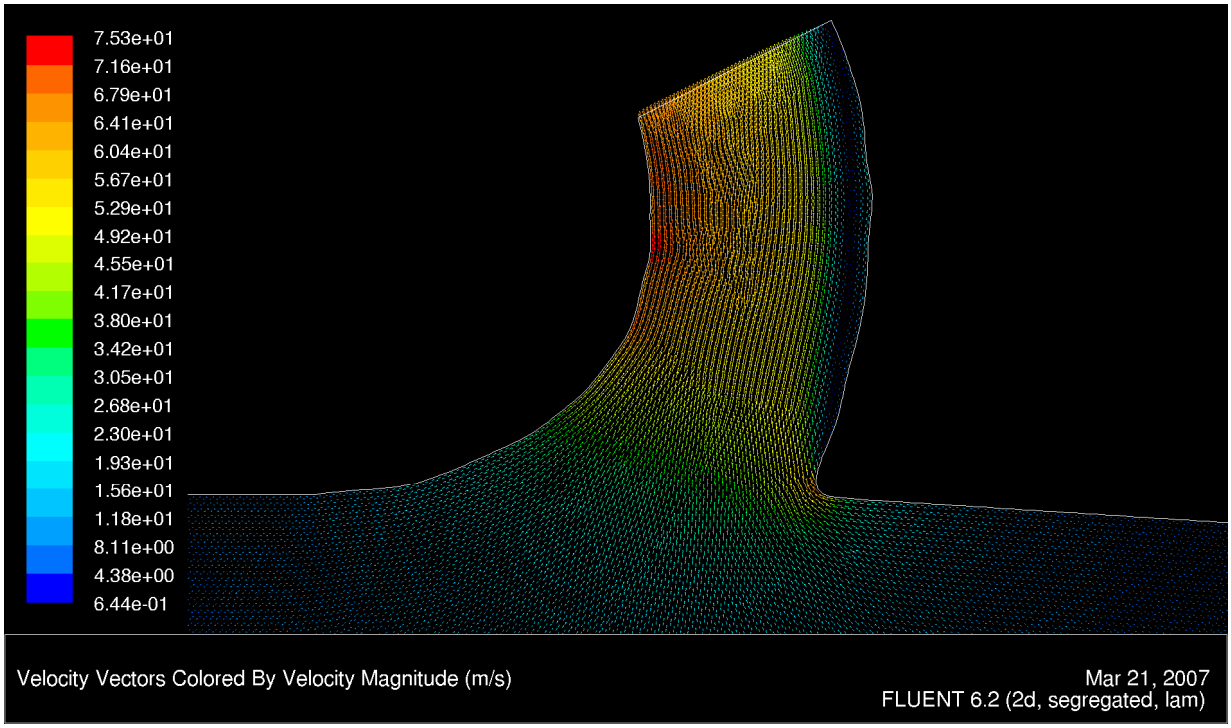

Figure 11: Rig model - velocity vectors in bleed

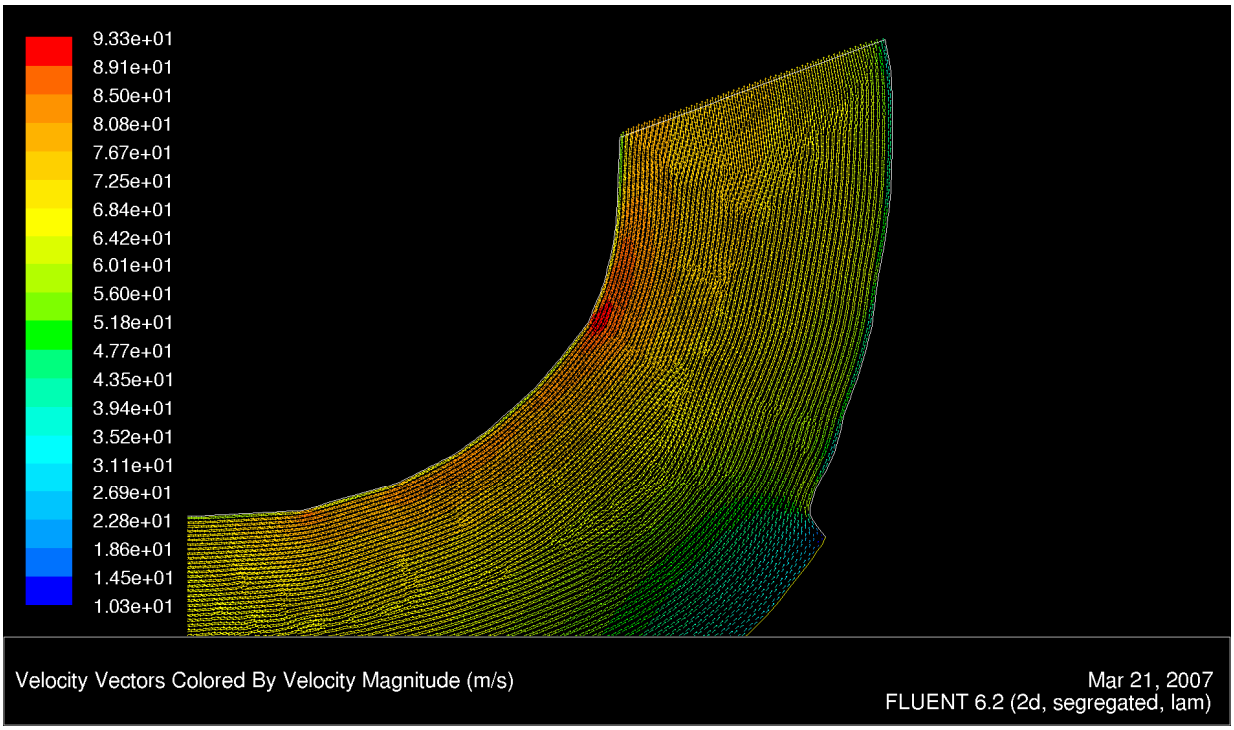

Figure 12: Engine model - velocity vectors in bleed

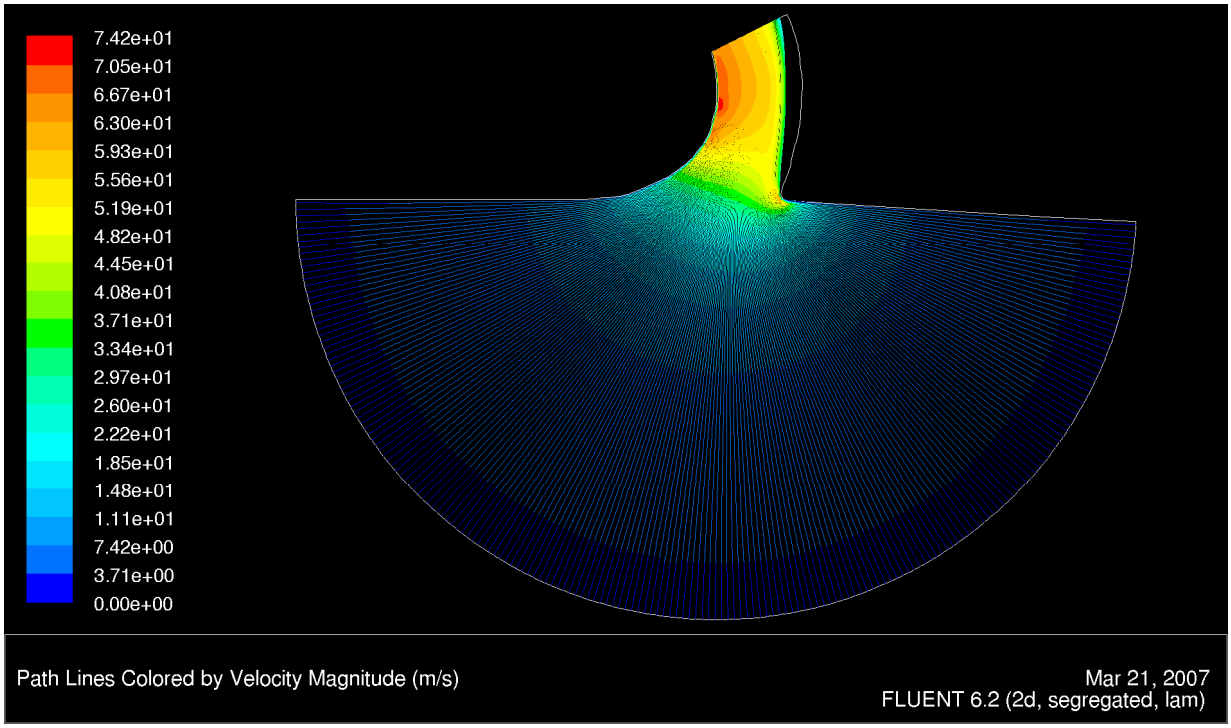

Figure 13: Rig model - streamlines colored by velocity magnitude

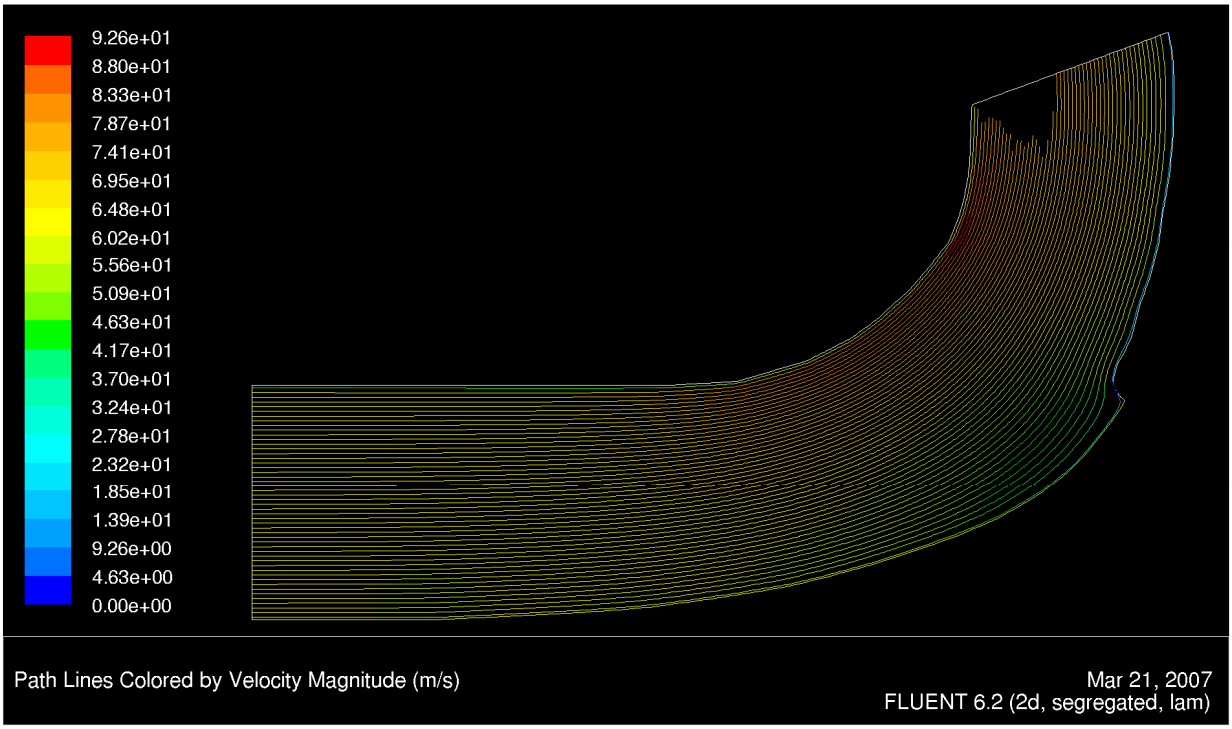

Figure 14: Engine model - streamlines colored by velocity magnitude

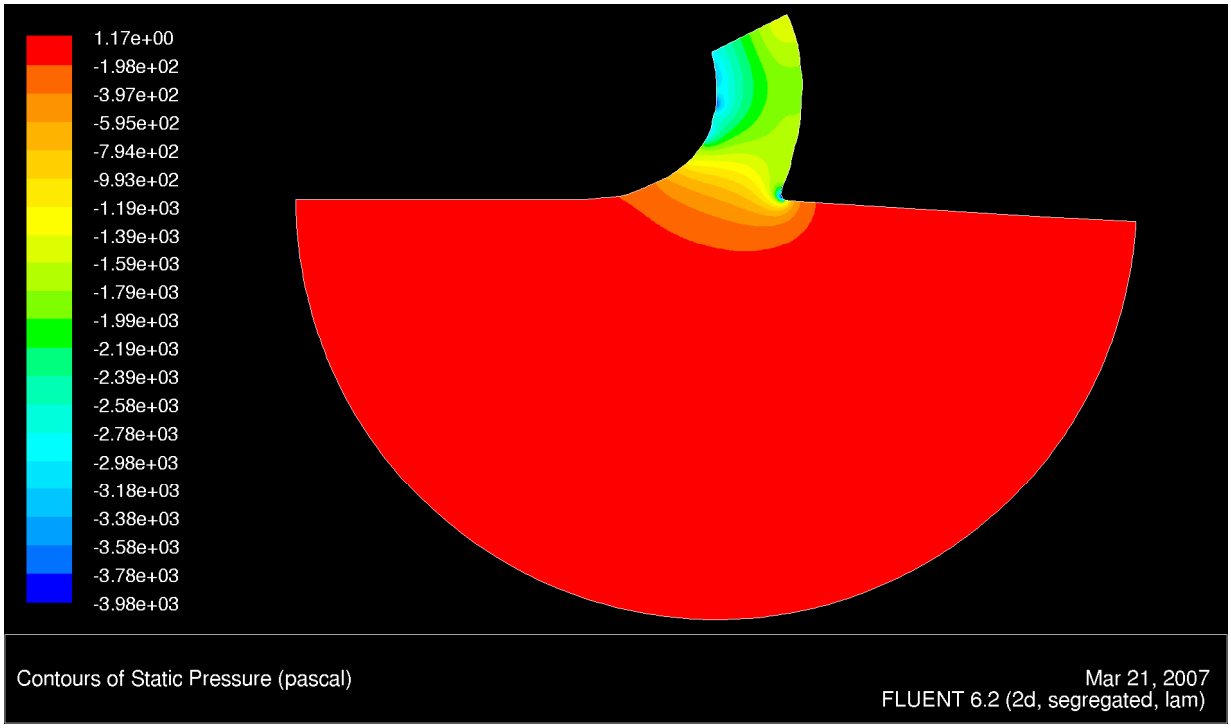

Figure 15: Rig model - static pressure contour plot

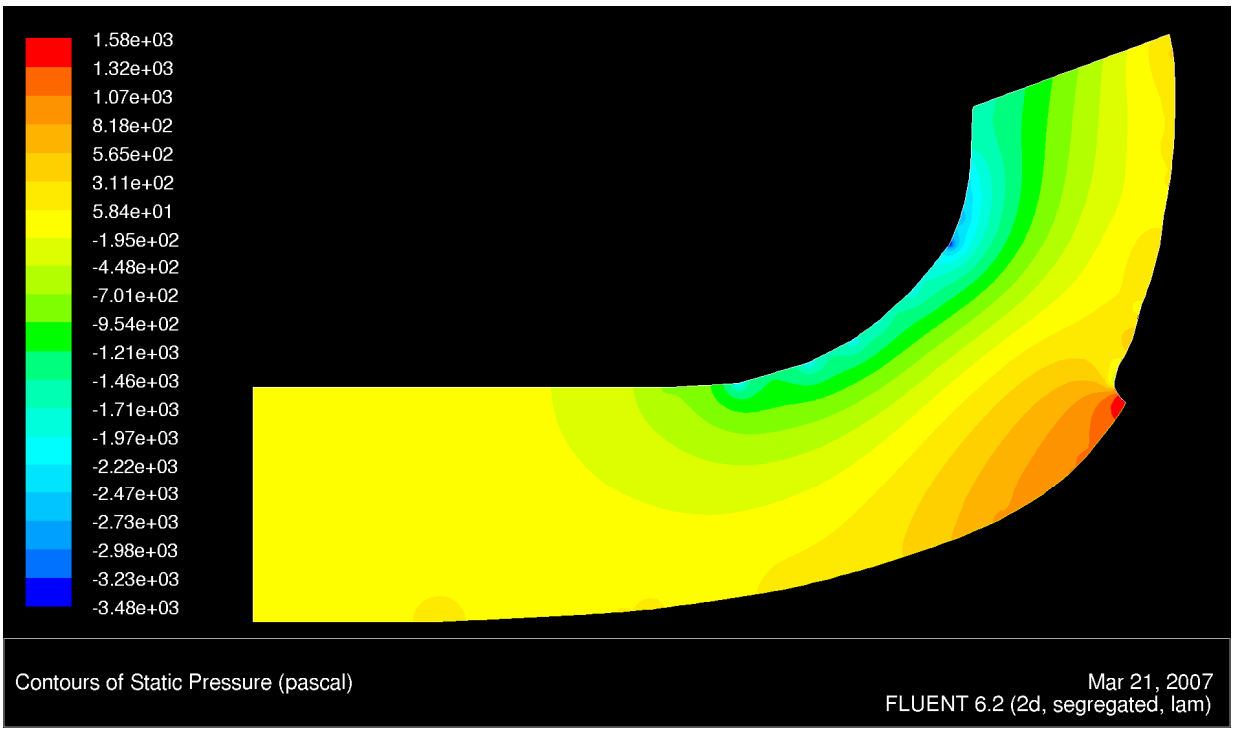

Figure 16: Engine model - static pressure contour plot

Data Validity Checks

Sink Flow Check

Prior to completing the more advanced Fluent models as seen above, a check was performed to give credence to the observed data. A previous rig flow solution was compared to an idealized sink flow. For a perfect sink, fluid velocity varies as the inverse of distance from the sink. To complete this check, y-components of velocity were exported from Fluent along a line from the bleed to the hemispherical boundary as shown in Figure 17. These y-components of velocity were plotted against distance, r, from the bleed and compared to a graph of 1/r which sink flow theory predicts.

The results matched theory relatively well and can be seen below in Figure 18. The rig obviously does not model sink flow perfectly since the bleed has a finite size to it. A perfect sink would be an infinitesimally small point which pulls fluid into it. The bleed and vacuum however, closely resemble this and we have determined that our data is valid due in part to this similarity.

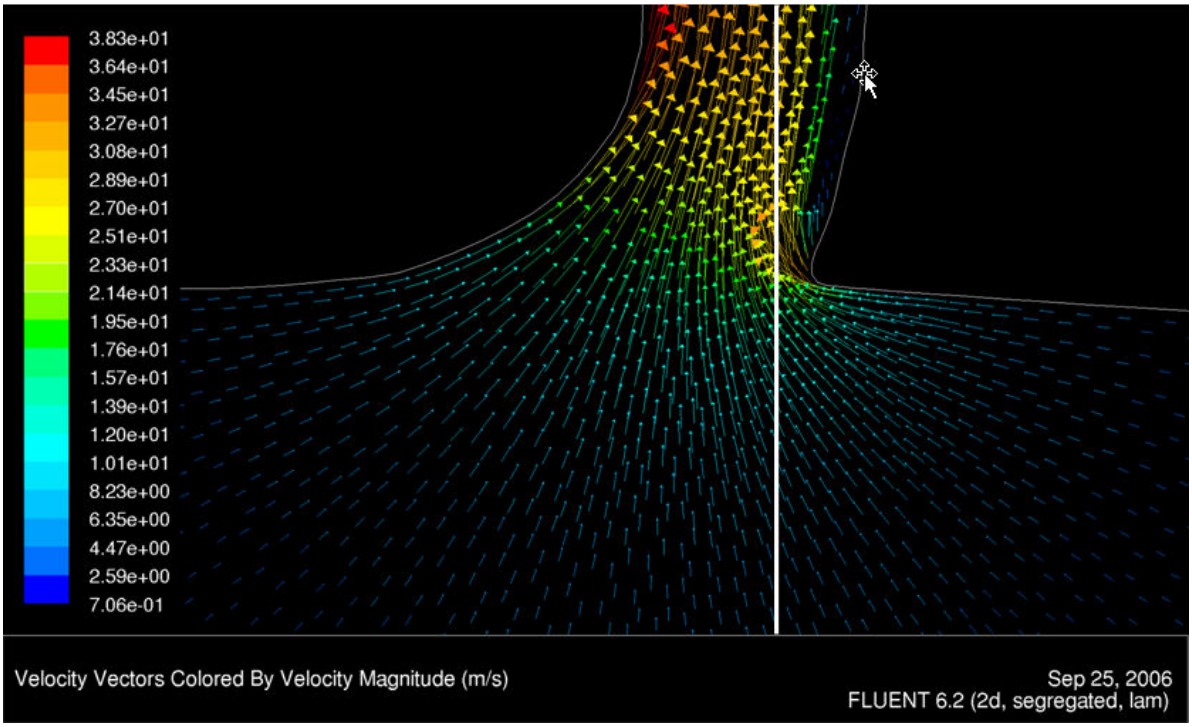

Figure 17: Line from bleed to hemispherical boundary

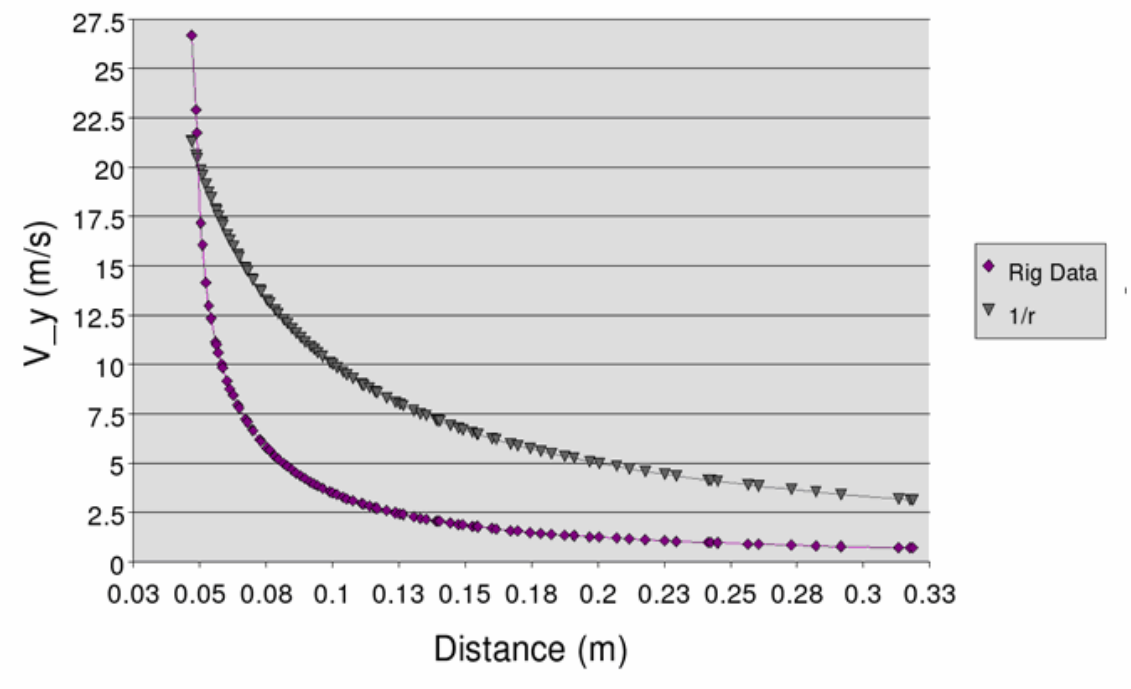

Figure 18: Plot of vertical (Y-direction) velocity versus distance from bleed

Grid Validity Check

In order to determine if the grid size used in the Fluent models was fine enough to produce accurate results, grid resolution was decreased for an older engine model. The velocity flow fields produced by these coarse grids were compared to that of the final grid resolution used. As can be seen in Figure 19, the flow fields produced are very similar. Based on these results, it was determined that the grid resolution being used in the final models was sufficient. As it turns out, more data points were needed to be used later in the particle trajectory code, so an extremely fine mesh was used.

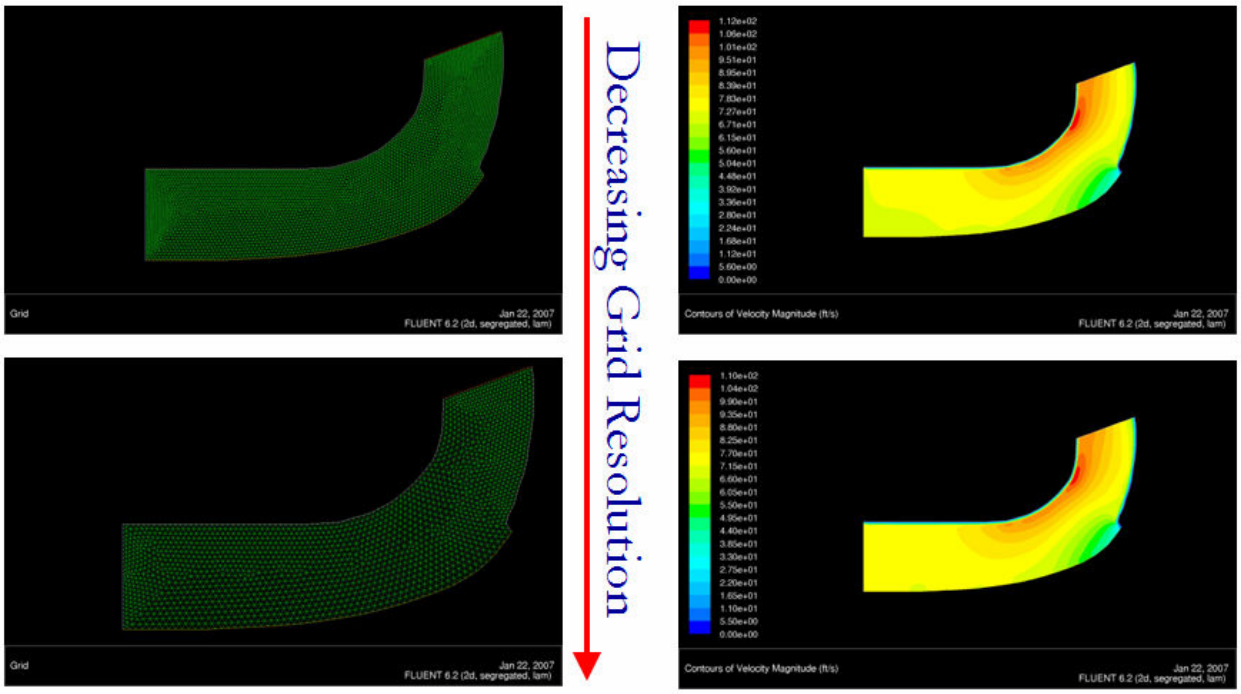

Figure 19: Velocity contours for varying grid sizes

Particle Trajectory Code

After computing the flow fields in Fluent for both the rig and engine, the next step was to determine how the flow fields influence the trajectory of an ingested hail particle. Although Fluent is capable of performing such calculations, creating a separate code allowed for a final product which was much more versatile and applicable to a broad range of similar problems with only minimal modifications. Because it is user friendly and widely used, Matlab version 2006a was selected as the programming language.

Initially, one code was written which only computed particle trajectory in the engine flow field domain. After debugging and extensive testing to ensure proper function, it was a simple task to modify the existing code to make it applicable to the rig domain. There are two separate and independent Matlab codes; one for the engine flow field and one for the rig flow field.

Once the flow field has been solved in Fluent, the values at grid nodes and the Cartesian coordinates of each node were exported as a text file in a matrix configuration. Of primary interest were the values of the velocity vectors (magnitude and direction) at each node. This information can be used to calculate the aerodynamic forces experienced by a particle as it is passing through the flow field.

Equation 1 is the drag force equation where c_D is the coefficient of drag, ρ is the density of the fluid, V_R is the relative velocity of the particle in the fluid, and A is the cross-sectional area of the particle.

$$\Sigma F = \left(c_D \rho \frac{V_R^{\,2}}{2} A \right) \tag{1}$$

Using Newton's second law, the drag force equation can be rearranged to solve for acceleration explicitly as in equation 2. In equations 3 and 4, the acceleration equation is

integrated to find velocity and position. These equations are solved using Matlab ODE45 solver in the particle trajectory code.

$$a = \frac{\left(c_D \rho \frac{V_R{}^2}{2} A \right)}{m} \tag{2}$$

$$\frac{dV_p}{dt} = \frac{\left(c_d \rho \frac{V_R^2}{2} A \right)}{m} \tag{3}$$

$$\frac{d^2 X_p}{dt^2} = \frac{\left(c_d \rho \frac{V_R^2}{2} A \right)}{m} \tag{4}$$

In the particle trajectory code, the only aerodynamic force considered is that of drag force. Brownian motion and other such effects were neglected because the size of these forces is several orders of magnitude smaller than the drag forces. Rapidly spinning spherical objects are subject to aerodynamically induced lift, however, in the case of hail traveling though the bleed it is unlikely that such effects will occur in any systematic fashion. Therefore, aerodynamic effects due to particle rotation were deemed beyond the scope of this project. Gravitational forces were also neglected. Gravitational effects were originally included but were subsequently removed after it was determined that these forces were also strongly dominated by aerodynamic effects.

Figure 20 shows a graphical illustration of the sequence of operations followed by the particle trajectory code. The majority of the calculations occur within the loop as seen in the figure. Typical number of iterations for a particular trajectory calculation are on the order of 100 and typical code runtime is approximately 10 seconds on a dual-core processor computer.

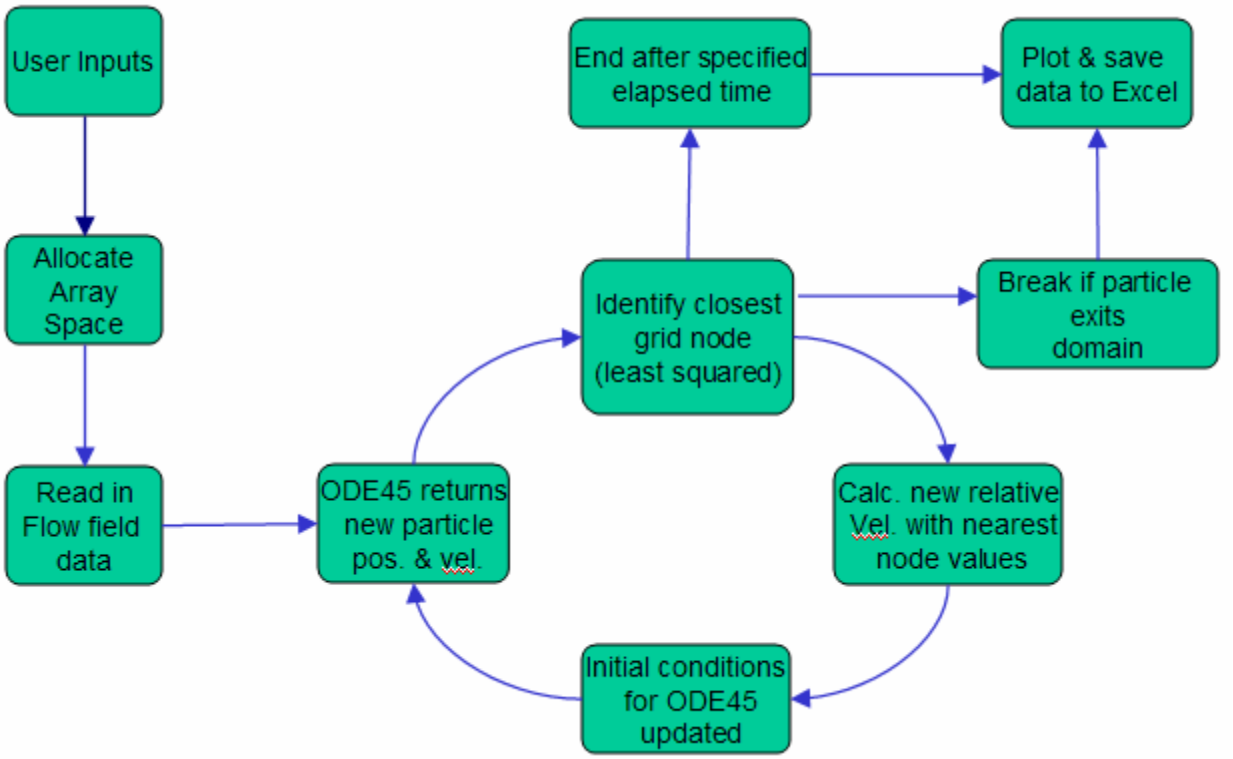

Figure 20: Matlab code execution sequence

The coefficient of drag was determined from studies performed on spheres at different Reynolds numbers. The standard Reynolds number vs. coefficient of drag relation can be seen in Figure 21. Analytical calculations were used to determine the maximum and minimum Reynolds numbers relevant to this project.

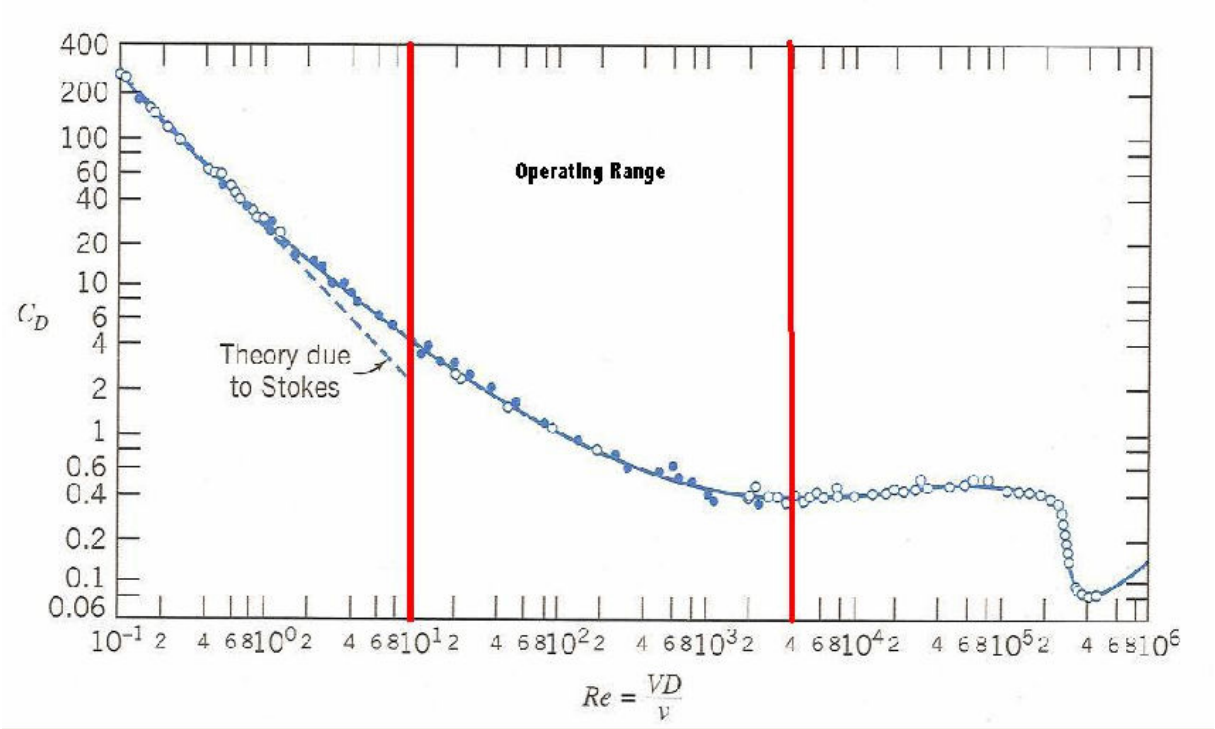

Figure 21: Operating Reynolds Number Range from 10 to 4000

The highly non-linear characteristics of the above relation meant that determining an equation for the line was extremely difficult. For this reason, the function was broken down into approximately 10 segments, and the equation for each segment was determined using a regression function in MS Excel. At each time step in the particle trajectory code, the Reynolds number is calculated using the following relation:

$$\mathrm{Re} = \frac{\rho V d}{\mu} \tag{5}$$

Based on the Reynolds number calculated, the coefficient of drag is found using the appropriate segment of the piecewise Re vs. c_D function.

The predicted coefficient of drag for a given Reynolds number was plotted against the actual values in Figure 22. The predictions coincide well with their real counterparts.

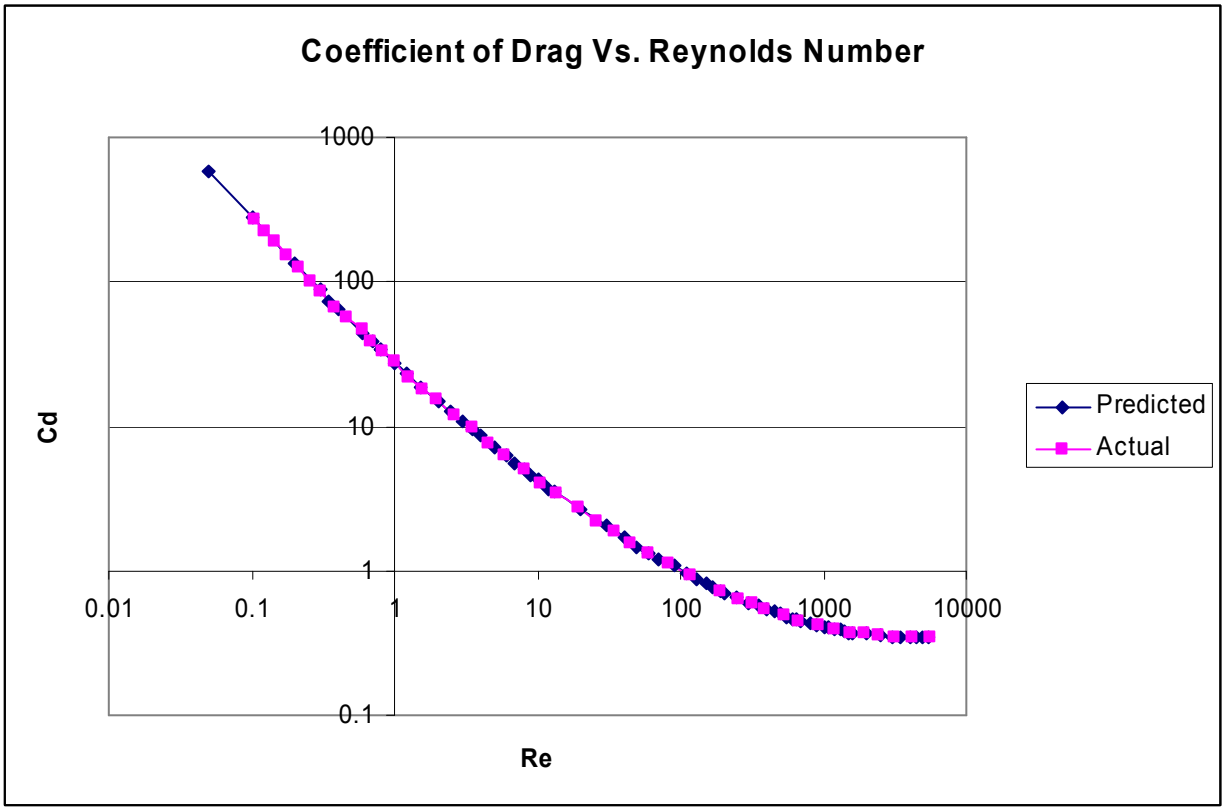

Figure 22: Comparison of Actual and Predicted Cd vs. Re

It is the velocity of the particle *relative* to the velocity of the air which dictates the force exerted on the particle by the fluid, and consequently the change in trajectory of the particle. For a particle moving at a velocity other than the precise velocity of the fluid, the relative velocity is constantly changing as the particle either speeds up or slows down due to drag forces. As previously described, the drag force equation was used to find the acceleration experienced by a particle over a differential time segment. Integration of this relation is used to find velocity, and double-integration is used to determine particle position.

The dlmread command is used to read-in fluid flow velocity text file that was exported from Fluent. At small time step increments (about .1 milliseconds), Matlab's ODE45 solver is used to perform a double integration of the drag force equation across each time step. ODE45

returns the new particle position and velocity in the x and y directions after that tiny time step. ODE45 uses a Runge-Kutta discretization method to solve Ordinary Differential Equations.

Using the new velocity and position data, the code finds the grid point which is closest to the particle in a "least squared" fashion using the distance formula. Then, the code retrieves the fluid velocity data for that grid point and uses those values to determine the *new* relative velocity between the particle and fluid. This *new* relative velocity is returned to the top of the loop and the process is repeated for the next time step. This process is repeated as the particle moves through the flow field. It is possible to use multiple node values to find the forces acting upon a particle; however this only becomes useful for particles several times larger than the cells. In this case the average particle size is less than twice that of the average cell, so it was decided not to use multiple cells in the calculations.[10]

The trajectory code is set to end after a user-specified time interval. However, the code will end if the particle crosses any of the domain boundaries such as the stagnation streamline, or bleed wall.

After the code has finished running, Matlab returns several pieces of information to the user. First, a graph is generated which displays the hail particle trajectory, allowing the user to "see" the trajectory of the particle during the run. Second, the code returns several MS Excel files containing the x and y position coordinates of the particle at every time step. Finally the initial settings for the run are saved in an Excel file. This data is helpful if the user wishes to recreate a certain run.

The figures below show typical graphs returned at the end of a single run of the code. The blue lines represent the domain geometry boundaries of the station 2.5 bleed in the engine and rig, respectively. The red line is a time series representation of the particle path as the particle progressed through the flow field.

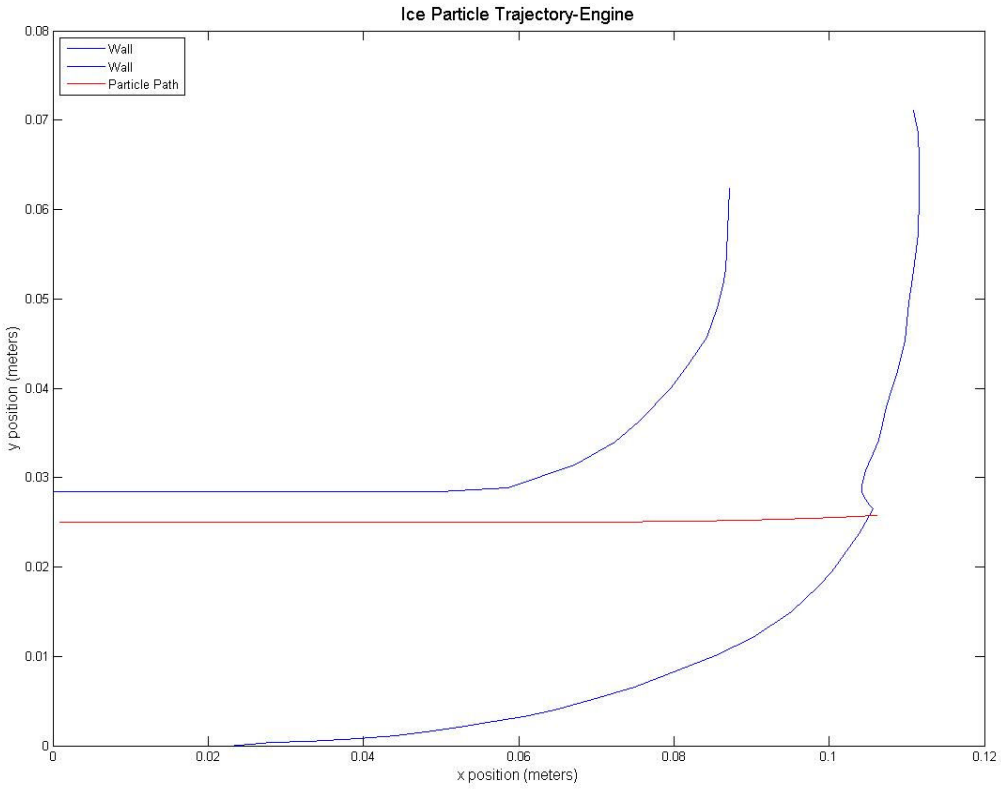

Figure 23: Particle Trajectory Sample Run-Engine

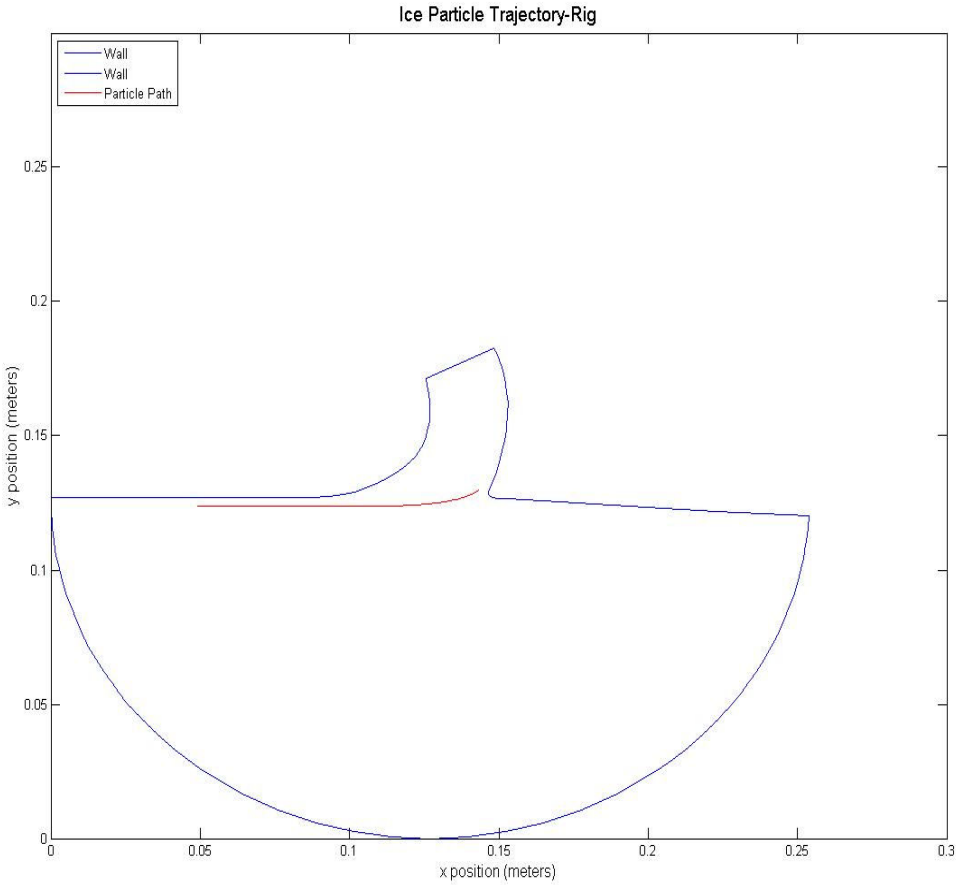

Figure 24: Particle Trajectory Sample Run-Rig

The accuracy of this iterative process is strongly related to the number of data points (grid points), and size of the time step. The default time step was determined by experimentally determining the limit past which the particle trajectory solution did not change.

Results

Upon completing several trajectory code runs for multiple input parameters, trends in the data became apparent. Data was collected which allowed direct comparison between performance of the engine and rig. To verify the code output a rough analytical analysis was performed using a number of simplifications.

The results shown in Figure 25 indicate that ballistic effects dominate over aerodynamic effects in the determination of hail particle trajectory. Aerodynamic effects do, however, produce substantial deflection of small diameter particles in the rig model. This result was most pronounced for .005 inches diameter particles which experienced a deflection of about .36 inches in the rig model and about .03 inches in the engine model. Please note that some of the following figures use logarithmic scales.

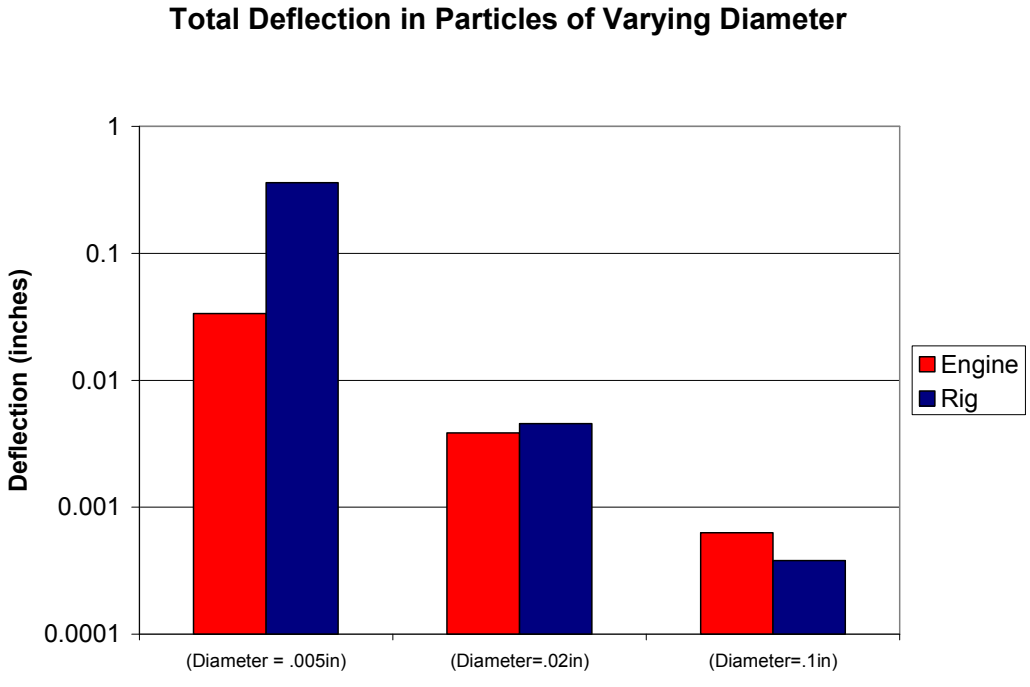

Figure 25: Total Deflection in Particles of Varying Diameter

In Figure 26, the geometries of the engine and rig have been superimposed in order to visually display the very interesting results of deflection at low particle diameters. The engine code and rig code were run using the same set of input parameters. The rig flow field caused particle deflections a whole order of magnitude larger that those generated by the engine's flow field for the same test. In general, for particles of diameter approximately .025 inches or smaller the rig model outperformed the engine model producing greater aerodynamically induced deflection.

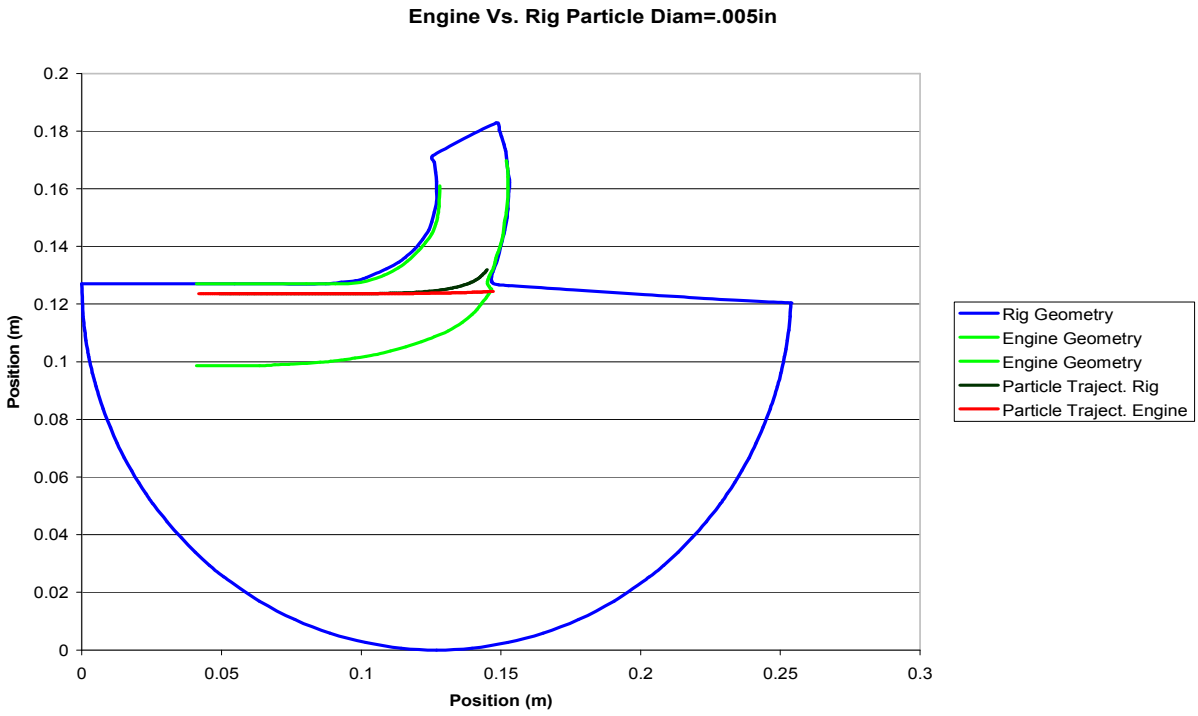

Figure 26: Engine Vs. Rig for Small Particle

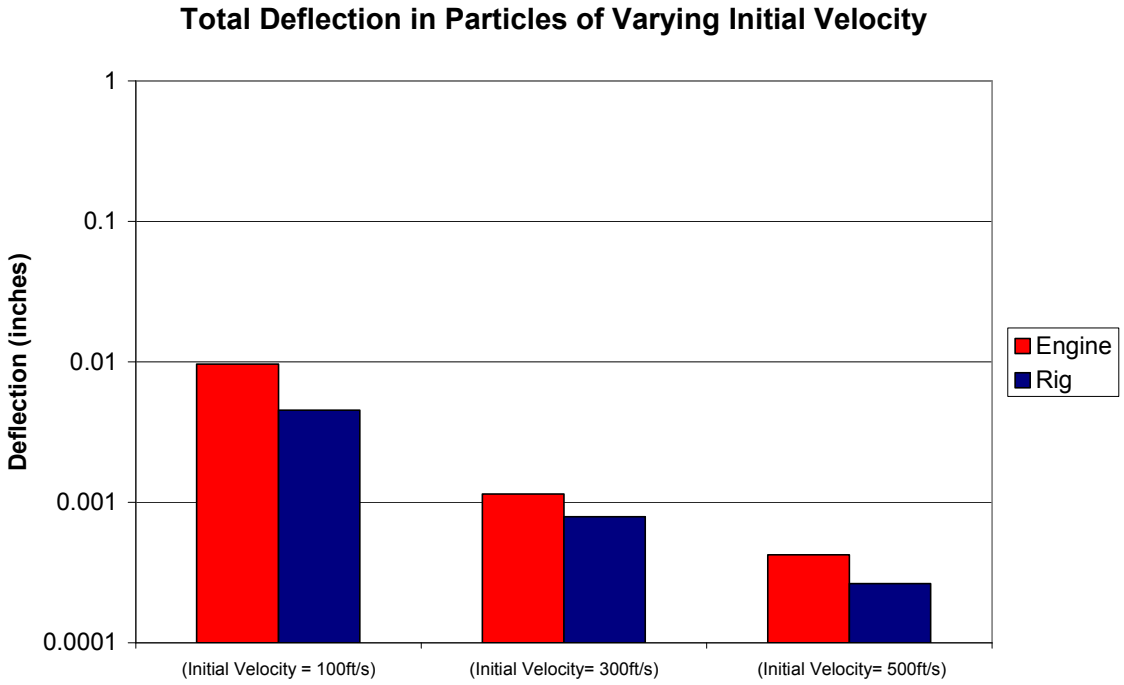

Figure 27: Total Deflection in Particles of Varying Initial Velocity

In Figure 27, the effect of varying the hail particle's initial velocity is presented. It is observed that the engine model deflection slightly exceeded that of the rig model across the entire range of initial speeds.

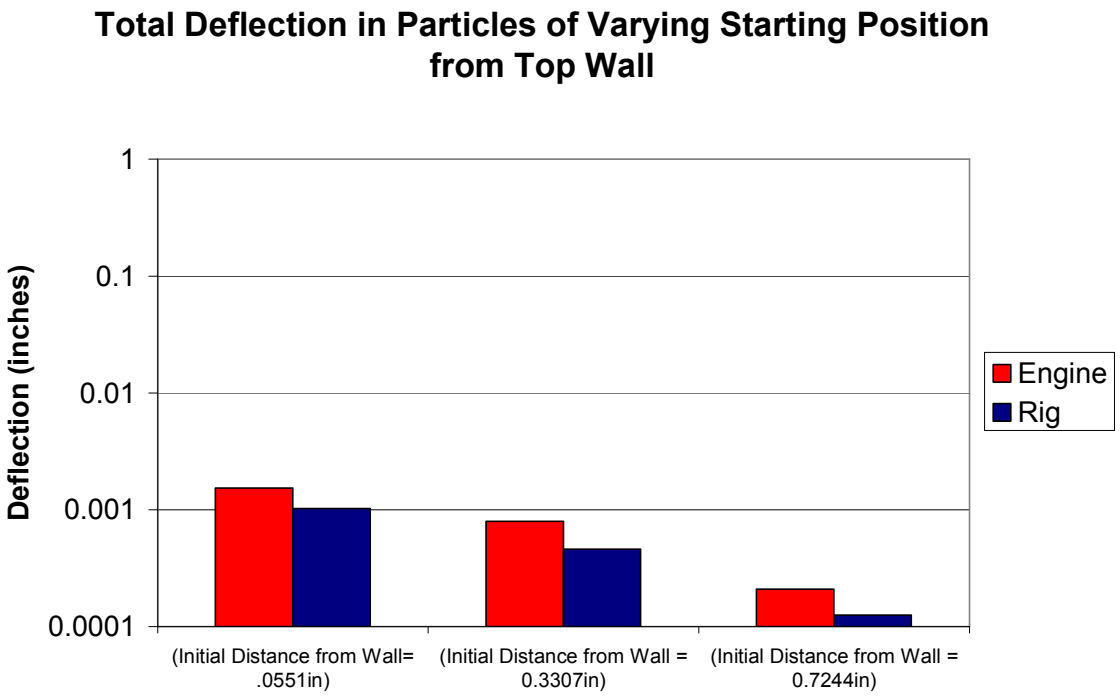

Figure 28: Total Deflection in Particles of Varying Starting Position from Top Wall

In Figure 28 the effect of hail particle starting position is studied. It shows that particles injected near the wall, where y-velocity is higher, experience greater deflection as expected. Particles in the engine experience greater deflections than those in the rig as well.

Analytical Comparison

In order to validate the range of deflections predicted by the Matlab trajectory code, analytical calculations were performed using the analytical model detailed below.

Figure 29 shows the y-velocity magnitude contour plot. A datum line was drawn .15 inches from the top wall which is a typical distance at which a particle is injected. The y-velocities at 20 points along this datum line were estimated and averaged, giving an average y-velocity (V_y = 21.3 ft/s) used in the equation shown below. Based on a typical particle speed of 72.3 ft/s, the particle residency time (Δt) came out to be .004545 seconds. Coefficient of drag (c_d) was taken to be 0.5, ρ_{air} = .0561 lbm/ft^3 based on engine conditions at 15,000 ft., ρ_{ice} = 49.95 lbm/ft^3, and an average particle diameter of .005 inches was used.

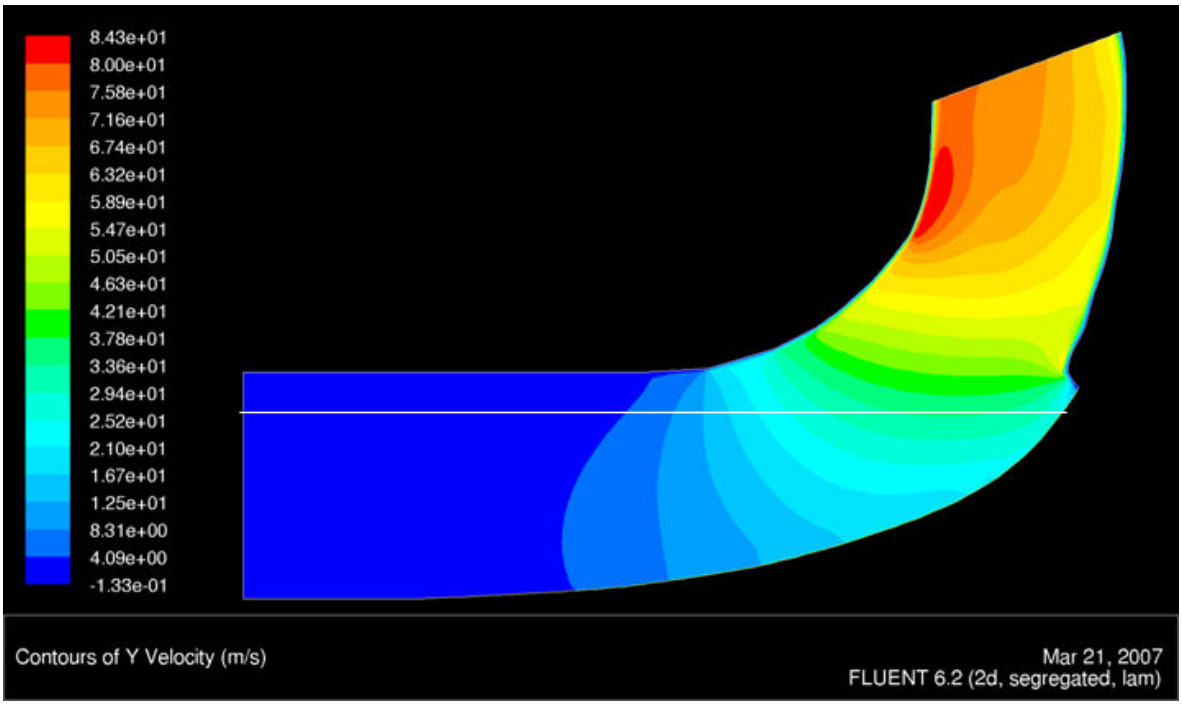

Figure 29: Y-velocity contour plot with datum line

The following acceleration equation was used in calculating deflection:

$$a = \frac{\left(c_D \rho \frac{V_R^{\,2}}{2} A \right)}{m} \tag{6}$$

Assuming a constant acceleration, the deflection can be approximated as $0.5a\left(\Delta t^2\right)$. Combined with the equation stated above, the following equation is produced.

$$deflection = \frac{d^2\left(\pi/16\right)c_d\rho_{air}V_y^2\left(\Delta t\right)^2}{\rho_{ice}\left(4\pi/3\right)\left(d/2\right)^3} \tag{7}$$

Figure 30 shows how numerical results obtained using the Matlab code compare to those predicted using the analytical methods. Identical input parameters were used in the Matlab code as in calculating the analytical deflection. The analytical solutions were rough and based and a number of simplifications, nevertheless, the two solutions were well within the same order of magnitude.

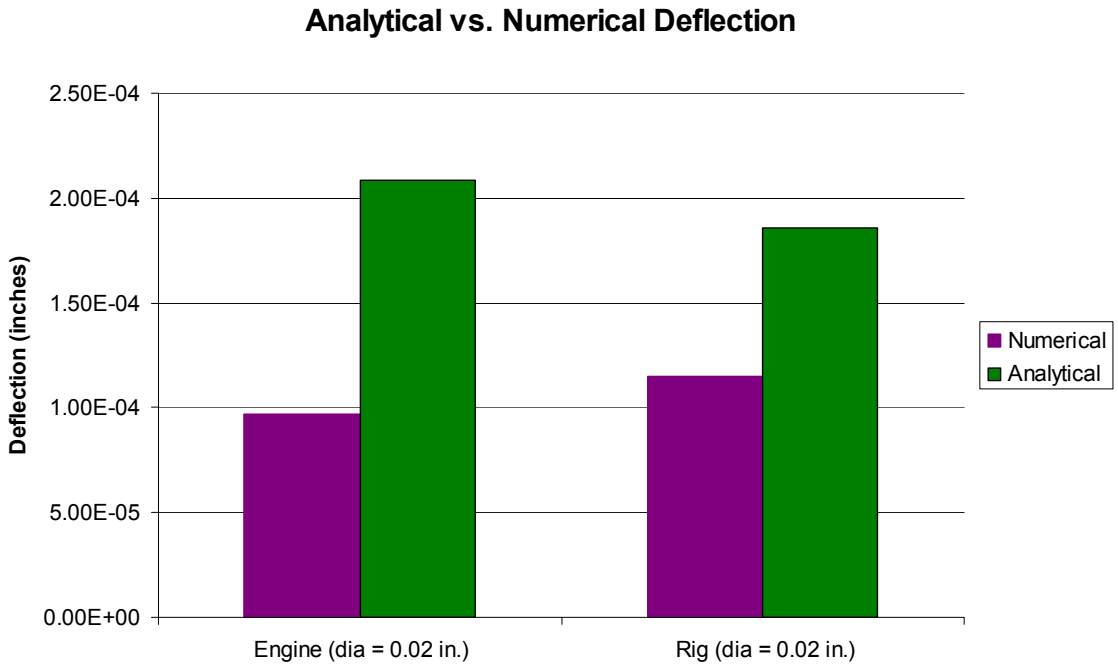

Figure 30: Analytical vs. Numerical Deflection

Conclusions

The primary result of the investigation was that the flow field in both the engine and rig did not significantly affect the ice particle trajectory. In other words, the hail follows a ballistic trajectory. Even in "worst case scenario" conditions where the properties of average size particles were set to cause as much deflection as plausible, the deflections were on the order of a hundredth of an inch. Even considering the small size of the bleed this size deflection is not going to greatly change the amount of particles entering the bleed. The only particles to encounter significant deflections were those with diameters on the order of thousandths of an inch. These larger deflections occurred only in the rig setup, so it would appear that the rig would take in more small particles than the engine.

Though larger deflections were expected at first, considering the high speeds and short distance the particles are in the influence of the bleed, there simply isn't enough time for most particles to be affected.

There were a few variables that did affect the final deflection amounts. Increased proximity to the bleed by traveling along the wall leading to the bleed increased the deflection because the particles traveled through an area with higher y velocities. Slower initial speeds allowed enough time for the particle to be affected more. Lighter particles also experience much more deflection because they have a smaller mass to cross-sectional area ratio. The mass increases with the cube of particle diameter, d, while the area increases with the square of the diameter, so the total acceleration and therefore, total deflection varies as 1/d as shown in the equation below. As a result, smaller diameter particles are deflected more.

$$a = \frac{C_d \frac{\rho_{air}}{2} V_{Rel}^2 A}{m} = \frac{d^2 \left(\pi/8\right) c_d \rho_{air} V_y^2}{\rho_{ice} \left(4\pi/3\right)\left(d/2\right)^3} \sim \frac{1}{d} \tag{8}$$

All the particles were modeled as smooth spheres. However, hail chips are likely to not be spherical. To make sure that larger coefficients of drag associated with non-spherical shapes would not change the particle trajectory significantly the code was run for common particle values and a high coefficient of drag. The highest likely coefficient of drag for the spherical hail is about 1.5. With c_d set to 1.5 the deflection was only a few times larger than the deflection of the spherical particle; which was already an extremely small amount. To further prove that the effect of varying c_d was not significant, the c_d was set to an extremely high value of 15. Even then the deflection was only about .1 inches, still very small in relation to the bleed size.

Future Work and Recommendations

Though it is believed that the work presented within this report is sound, there are certain subjects that were not possible to fully investigate due to time, lack of information, and limited resources. In the event that a future group continues this project, some potential improvements have been listed.

The hail entering the bleed was approximated as a sphere. Though it was shown that even larger coefficients of drag did not change the trajectory significantly, the fact still remains that the ice entering the bleed will likely not be spherical. Rough spheres and other shapes were studied to see if there was a difference in the coefficient of drag. Studies on the shape of the actual particles could lead to a better way to approximate the coefficient of drag. This could lead to more accurate predictions, though the work shows that the effect will probably be small.[11]

Because the coefficient of drag on a sphere is directly related to the Reynolds number, the code relates the two properties. Within the particle trajectory code, x and y-direction ODE operations are decoupled for programming simplicity. Consequently, the Reynolds number for x and y-direction flow are calculated independently. Whether or not this creates any problems is unknown. There appears to be no change depending on whether or not the Reynolds number is decoupled or based on the total velocity. Further investigations may be needed to resolve this question.

Adding hail particle interactions with the solid walls would be another way to improve the realism of the code. This group had neither the time nor experience with CFD modeling to properly compute what will happen to the particle when it hits the wall. For the most part, it was assumed that a particle impinging upon a wall will remain along the wall. Better models might

include the ability to simulate particle interaction with a wall and/or calculate how the ice will shatter and break apart.

Compressibility effects could also be included in the Fluent. Because all air speeds were less than Mach 0.3, compressible effects should be minimal. Despite attempts to model with compressible effects added, the boundary conditions applied in Fluent did not allow for this. Different boundary conditions could also be applied in Fluent.

The difficulty in obtaining engine conditions could also affect accuracy. The conditions for the area around the bleed were taken from computer models of the engine. These conditions are not necessarily the same as the conditions close to the bleed. In the Fluent models it was found that the trajectory of the particles was influenced specifically by the air density and other properties.

Turbulence modeling could also be included in the Fluent model. There are multiple turbulence models that can be used in Fluent such as a k-epsilon model. Turbulence models used in the Fluent models will very likely affect the flow field however it has already been shown that aerodynamic effects have little influence on the hail particle trajectories except at low diameters.

Lastly, using a three-dimensional model might reveal behavior that were not seen in the two-dimensional Fluent models. However, using three-dimensional models would significantly increase the complexity of the Matlab code and the modeling in Fluent.

There were many other effects which we did not fully investigate. Spinning particles might produce pressure gradients, creating lift that may change the particle's trajectory. The air entrained by the large diameter particles might also affect surrounding ice particles. The difference in airflow velocity over the particle's surface might also change the results, though research seems to say this is a limited effect for particles of the sizes used.

An underlying assumption on this project was that one hail particle would be traveling through the flow fields in both the engine and rig models. In actual hail storms and rig simulations, a large quantity of hail is passing through the flow field. These particles may or may not affect the flow field. The effect of the interaction between the particles and the flow field is beyond the scope of this project but worthy of further investigation.

None of these effects should change the main result of the work. The trajectory of the particles is mainly ballistic. Accuracy might be improved by including the aforementioned effects, but it will probably not change the findings overall.

As well as investigating possible improvements to the code, those who wish to further this project may study particles with an initial y-velocity. The main object of the investigation was to study the effects of the airflow on particles moving parallel to the rig/engine flow. Future work may involve studying the deflections of a particle with an initial y-velocity.

Reference List

[1] "Bleeding Hearts," *Cockpit Conversation* [online], 16 June 2005, http://airplanepilot.blogspot.com/2005/06/bleeding-hearts.html [retrieved 12 October 2006].

[2] Holladay, A., "Operating Jets in the Rain," *WonderQues* [online], 16 May 2001, http://www.wonderquest.com/JetsRain.htm [retrieved 14 October 2006].

[3] Jane, G. F., "Airworthiness Standards; Rain and Hail Ingestion Standards," *Federal Aviation Administration* [online database], 20 Mar. 1998, http://www.faa.gov/regulations_policies/rulemaking/historical_documents/1998/media/a23-53.pdf [retrieved 14 October 2006].

[4] Pan, H., and Render, P. M., "Experimental Studies Into the Hail Ingestion Characteristics of Turbofan Engines," *American Institute of Aeronautics and Astronautics* [online], Department of Aeronautical and Automotive Engineering, Loughborough University of Technology, 1994, http://pdf.aiaa.org/preview/1994/PV1994_2956.pdf [retrieved 13 October 2006].

[5] Urban, J., "Bleed Flow Effects On Ice Particles MQP," *United Technologies Corporation* [Microsoft PowerPoint presentation], 2006.

[6] "FLUENT 6.2 User's Guide," *Fluent Incorporated*, 2005

[7] Ahmadi, Goodarz, "Particle Transport and Deposition in the Hot-Gas Filter at Wilsonville," *Clarkson University* [online], 24 June 1999, http://www.osti.gov/bridge/servlets/purl/793319-sOMvph/native/793319.pdf [retrieved 28 March 2007].

[8] Albert, R.L. and M.K. Matthews, "Calculation of Large-Scale Flow Fields Induced by Droplet Sprays," *Factory Mutual Systems*, 1979.

[9] Fox, R. W., McDonald, A. T., and Pritchard, P. J., "External Incompressible Viscous Flow," *Introduction to Fluid Mechanics*, 6th ed., John Wiley & Sons, Inc., Hoboken, New Jersey, 2004, pp. 439.

[10] Agrawal, M., Bakker, A., Prinkey, M., "Macroscopic Particle Model Tracking Big Particles in CFD," *Annual Meeting Conference Proceedings*, AICHE, 2004, pp. 2623-2625.

[11] Achenbach, E., "Experiments on Flow Past Spheres," *Journal of Fluid Mechanics*, Volume 54, Part 3, 1972, pp. 565-575.

Appendices

Appendix A: Boundary Conditions

Properly specified boundary types are a critical step in creating a reliable Fluent simulation. Boundary types dictate the information supplied by the user in order for Fluent to solve for a particular flow field. The number of input parameters for a given boundary type varies for each type.

There are over 60 ways to define a boundary in Fluent. The important characteristics of some of the most popular types are summarized below. The "parameters to specify" are based on non-combusting, non-radiating, non-chemically reacting, single-phase flows.

Velocity Inlet boundary conditions are used to define the velocity and scalar properties of the flow at the inlet boundaries. Parameters to specify are as follows:

- Velocity magnitude and direction/vector components
- Swirl velocity
- Temperature
- Outflow gage pressure (for coupled solver)
- Turbulence parameters

Fluent uses both velocity components and their user-defined scalar quantities as boundary conditions to compute the inlet mass flow rate, momentum fluxes and fluxes of energy and chemical species. The mass flow rate entering a fluid cell adjacent to a velocity inlet boundary is computed as:

$$\dot{m} = \int \rho \vec{V} * d\vec{A}$$

Pressure Inlet boundary conditions are used to define the total pressure and other scalar quantities at flow inlets. Parameters to specify are as follows:

- Stagnation pressure and temperature
- Flow direction, vector components or normal to boundary
- Static pressure
- Turbulence parameters

When flow enters through a pressure inlet boundary, Fluent uses the user-specified boundary pressure as the total pressure of the fluid at the inlet plane. In incompressible flow, the inlet total pressure, Po, and the static pressure, Ps, are related to the inlet velocity via Bernoulli's equation:

$$p_o = p_s + \frac{1}{2}\rho V^2$$

In compressible flows, isentropic relations for an ideal gas are applied to relate total pressure, static pressure, and velocity as a pressure inlet boundary. Your input of total pressure, p_o', at the inlet and the static pressure, p_s', in the adjacent fluid cell are thus related as

$$\frac{p_o' + p_{op}}{p_s' + p_{op}} = \left(1 + \frac{\gamma - 1}{2} M^2\right)^{\frac{\gamma}{\gamma - 1}}$$

where $M = \frac{v}{c} = \frac{v}{\sqrt{\gamma R T_s}}$, c = the speed of sound, $\gamma = \frac{c_p}{c_v}$, and operating pressure is p_{op}.

Mass Flow Inlet boundary conditions are used in compressible flows to prescribe a mass flow rate at an inlet. It is not necessary to use mass flow inlets in incompressible flows because when density is constant, velocity inlet boundary conditions will fix the mass flow. Parameters to specify are as follows:

- Mass flow rate, mass flux, or average mass flux
- Stagnation temperature
- Static pressure
- Flow direction
- Turbulence parameters

There are two ways to specify the mass flow rate. The first is to specify the total mass flow rate, $\dot{m}$, for the inlet. The second is to specify the mass flux, ρv_n (mass flow rate per unit area). If a total mass flow rate is specified, Fluent converts it internally to a uniform mass flux by dividing the mass flow rate by the total inlet area:

$$\rho v_n = \frac{\dot{m}}{A}$$

If the inlet is supersonic, the static pressure used is the value that has been set as a boundary condition. If the inlet is subsonic, the static pressure is extrapolated from the cell inside the inlet face.

The static temperature at the inlet is computed from the total enthalpy, which is determined from the total temperature that has been set as a boundary condition. The total enthalpy is given by:

$$h_o(T_o) = h(T) + \frac{1}{2}V^2$$

Pressure Outlet boundary conditions are used to define the static pressure at the flow outlets (and other scalar variables, in case of backflow). The use of a pressure outlet boundary condition instead of an outflow condition often results in a better rate of convergence when backflow occurs during iteration. Parameters to specify are as follows:

- Static Pressure
- Stagnation temperature
- Backflow direction specification method
- Turbulence parameters

The static pressure value you enter is relative to the operating pressure set in the "Operating conditions panel."

Pressure Far-Field boundary conditions are used to model free-stream compressible flow at infinity, with free-stream Mach number and static conditions specified. This boundary type is available only for compressible flows. Parameters to specify are as follows:

- Static pressure
- Mach number
- Temperature
- Flow direction
- Turbulence parameters

The pressure far-field boundary condition is a non-reflecting boundary condition based on the introduction of Riemann invariants (i.e., characteristic variables) for a one-dimensional flow normal to the boundary. For flow that is subsonic there are two Riemann invariants, corresponding to incoming and outgoing waves:

$$R_{\infty} = v_{n\infty} - \frac{2c_{\infty}}{\gamma - 1}$$

$$R_i = v_{ni} + \frac{2c_i}{\gamma - 1}$$

where v_n is the velocity magnitude normal to the boundary, c is the local speed of sound and γ is the ratio of specific heats (ideal gas). The subscript "∞" refers to conditions being applied at infinity (the boundary conditions), and the subscript "i" refers to conditions in the interior of the domain (i.e., in the cell adjacent to the boundary face). These two invariants can be added and subtracted to give the following two equations:

$$v_n = \frac{1}{2}\left(R_i + R_\infty\right)$$

$$c = \frac{\gamma - 1}{4}\left(R_i - R_\infty\right)$$

where v_n and c become the values of normal velocity and sound speed applied on the boundary. At a face through which flow exits, the tangential velocity components and entropy are extrapolated from the interior; at an inflow face, these are specified as having free-stream values. Using the values for v_n, c, tangential velocity components, and entropy the values of density, velocity, temperature, and pressure at the boundary face can be calculated.

Inlet Vent/Outlet Vent boundary conditions are used to model an inlet vent with a specified loss coefficient, flow directions, and ambient (inlet) total pressure and temperature. An inlet vent is considered to be infinitely thin, and the pressure drop through the vent is assumed to be proportional to the dynamic head of the fluid, with an empirically determined loss coefficient that you supply. Parameters to specify are as follows:

- Stagnation pressure
- Stagnation temperature
- Flow direction

- Static pressure
- Turbulence parameters
- Loss coefficient

The pressure drop, ΔP, varies with the normal component of velocity through the vent, v, as follows:

$$\Delta P = k_L \frac{1}{2} \rho V^2$$

where ρ is the fluid density, and k_L is the non-dimensional loss coefficient.

Outflow boundary conditions are used to model flow exits where the details of the flow velocity and pressure are not known prior to solution of the flow problem. They are appropriate where the exit flow is close to a fully developed condition, as the outflow boundary condition assumes a zero normal gradient for all flow variables except pressure. You cannot use outflow boundaries if the following condition(s) apply:

- a problem includes pressure inlet boundaries; use pressure outlet boundary conditions (see Section 7.8) instead
- you are modeling compressible flow
- you are modeling unsteady flows with varying density, even if the flow is incompressible

In Fluent, it is possible to use multiple outflow boundaries and specify the fractional flow rate through each boundary. In the Outflow panel set the Flow Rate Weighting to indicate what portion of the outflow is through the boundary.

The **Flow Rate Weighting** is a weighting factor:

$$percentage\ flow through\ boundary = \frac{flow\ rate\ weighting\ specified\ on\ boundary}{sum\ of\ all\ flow\ rate\ weighting}$$

Intake fan/Exhaust fan boundary conditions are used to model an external intake fan with a specified pressure jump, flow direction, and ambient (intake) total pressure and temperature. An intake fan is considered to be infinitely thin, and the discontinuous pressure rise across it is specified as a function of the velocity through the fan. In the case of reversed flow, the fan is treated like an outlet vent with a loss coefficient of unity. Parameters to specify are as follows:

- Stagnation pressure
- Stagnation temperature
- Flow direction
- Static pressure
- Turbulence parameters
- Pressure jump

You can define the **Pressure-Jump** across the fan as a **constant**, **polynomial**, **piecewise-linear**, or **piecewise-polynomial** function of the normal velocity. The panels for defining these functions are the same as those used for defining temperature-dependent properties.

- **Wall** Boundary conditions are used to bound fluid and solid regions. Inviscous flows, the no-slip boundary condition is enforced at walls by default, but you can specify tangential velocity component in terms of the translational or rotational motion of the wall boundary, or model a “slip” wall by specifying shear.

- **Symmetry** boundary conditions are used when the physical geometry of interest and the expected pattern of the flow/thermal solution have mirror symmetry. They can also be used to model zero-slip shear walls in viscous flows. Note that at the centerline of an axisymmetric geometry, the axis boundary type should be used rather than the symmetry boundary type. Characteristics of s symmetry boundary are as follows:
    - Zero normal velocity at a symmetry plane
    - Zero normal gradient of all variables at a symmetry plane

- **Axis** is a boundary type that must be used as the centerline of an axisymmetric geometry (see Figure 31 below). You do not need to define any boundary conditions at axis boundaries. To determine the appropriate physical value for a particular variable at a point on the axis, Fluent uses the cell value in the adjacent cell.

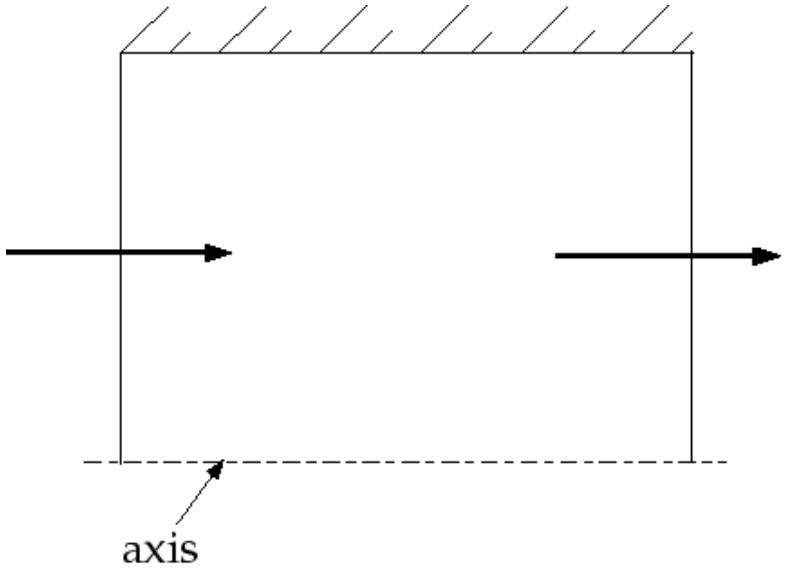

Figure 31: Axis Boundary Condition

Appendix B: Fluent Input Parameters

All parameters not shown below should be assumed to have been left at their default value.

Rig Input Parameters:

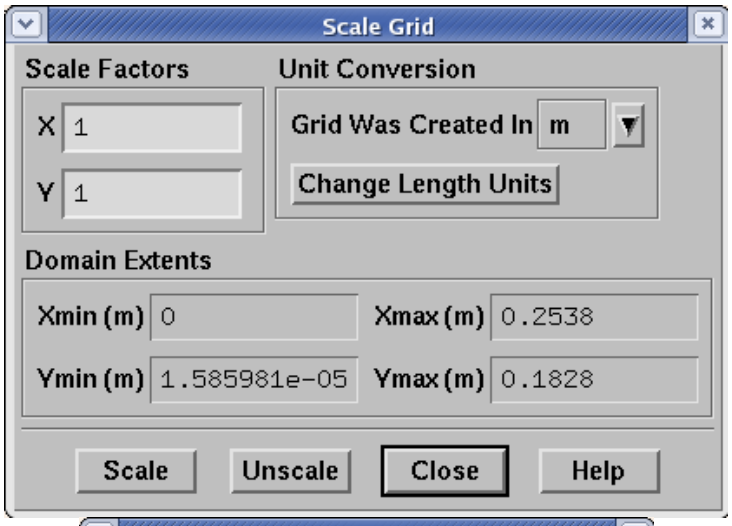

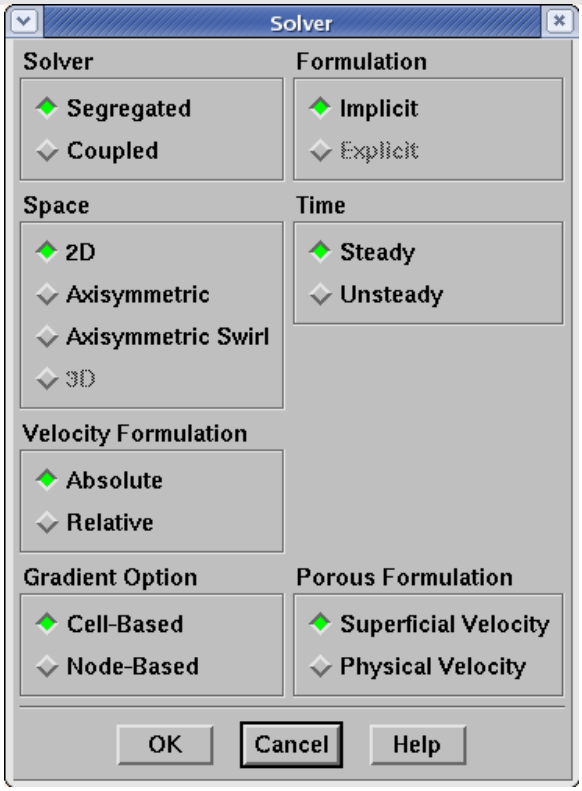

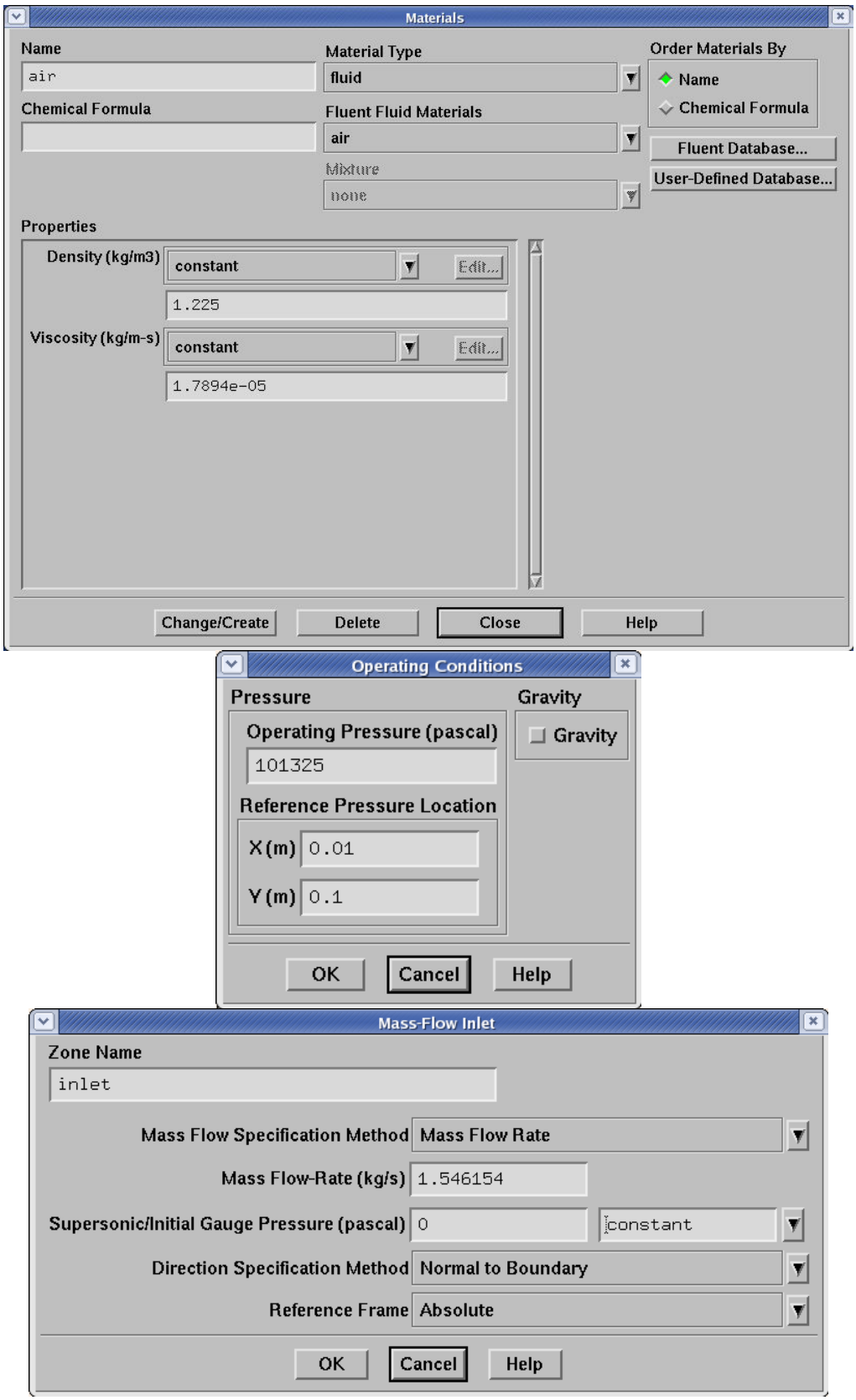
Materials
Name
air
Material Type
fluid
Order Materials By
Name
Chemical Formula
Chemical Formula
Fluent Fluid Materials
air
Fluent Database...
Mixture
none
User-Defined Database...
Properties
Density (kg/m3)
constant
Edit...
1.225
Viscosity (kg/m-s)
constant
Edit...
1.7894e-05
Change/Create
Delete
Close
Help
Operating Conditions
Pressure
Operating Pressure (pascal)
101325
Reference Pressure Location
X (m)
0.01
Y (m)
0.1
Gravity
Gravity
OK
Cancel
Help
Mass-Flow Inlet
Zone Name
inlet
Mass Flow Specification Method
Mass Flow Rate
Mass Flow-Rate (kg/s)
1.546154
Supersonic/Initial Gauge Pressure (pascal)
0
constant
Direction Specification Method
Normal to Boundary
Reference Frame
Absolute
OK
Cancel
Help

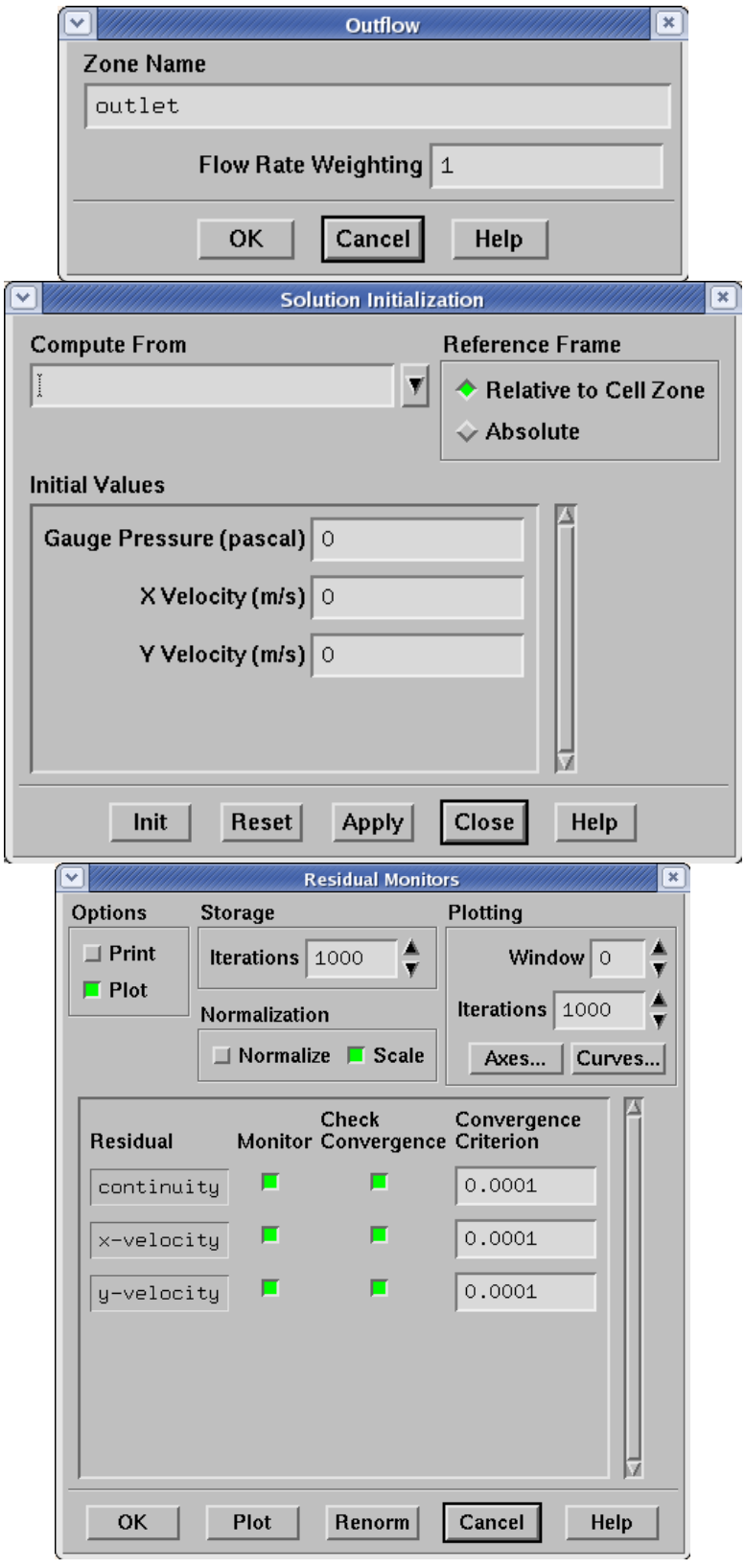
Outflow
Zone Name
outlet
Flow Rate Weighting
1
OK
Cancel
Help
Solution Initialization
Compute From
Reference Frame
Relative to Cell Zone
Absolute
Initial Values
Gauge Pressure (pascal)
0
X Velocity (m/s)
0
Y Velocity (m/s)
0
Init
Reset
Apply
Close
Help
Residual Monitors
Options
Print
Plot
Storage
Iterations
1000
Normalization
Normalize
Scale
Plotting
Window
0
Iterations
1000
Axes...
Curves...
Residual
Monitor
Check Convergence
Convergence Criterion
continuity
0.0001
x-velocity
0.0001
y-velocity
0.0001
OK
Plot
Renorm
Cancel
Help

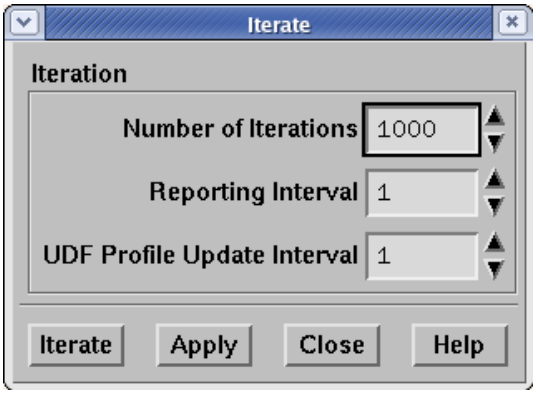

Engine Input Parameters:

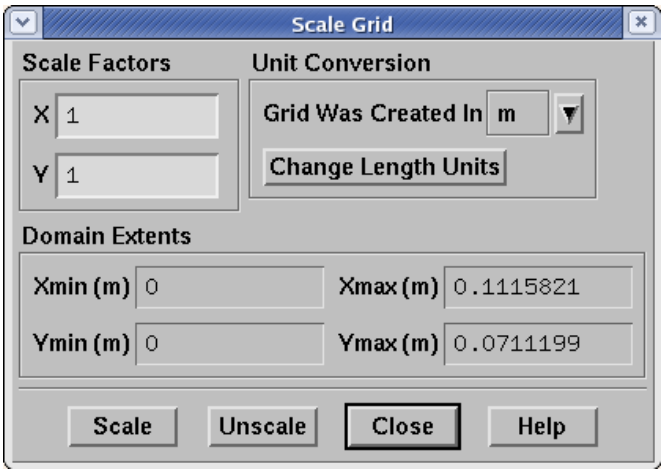

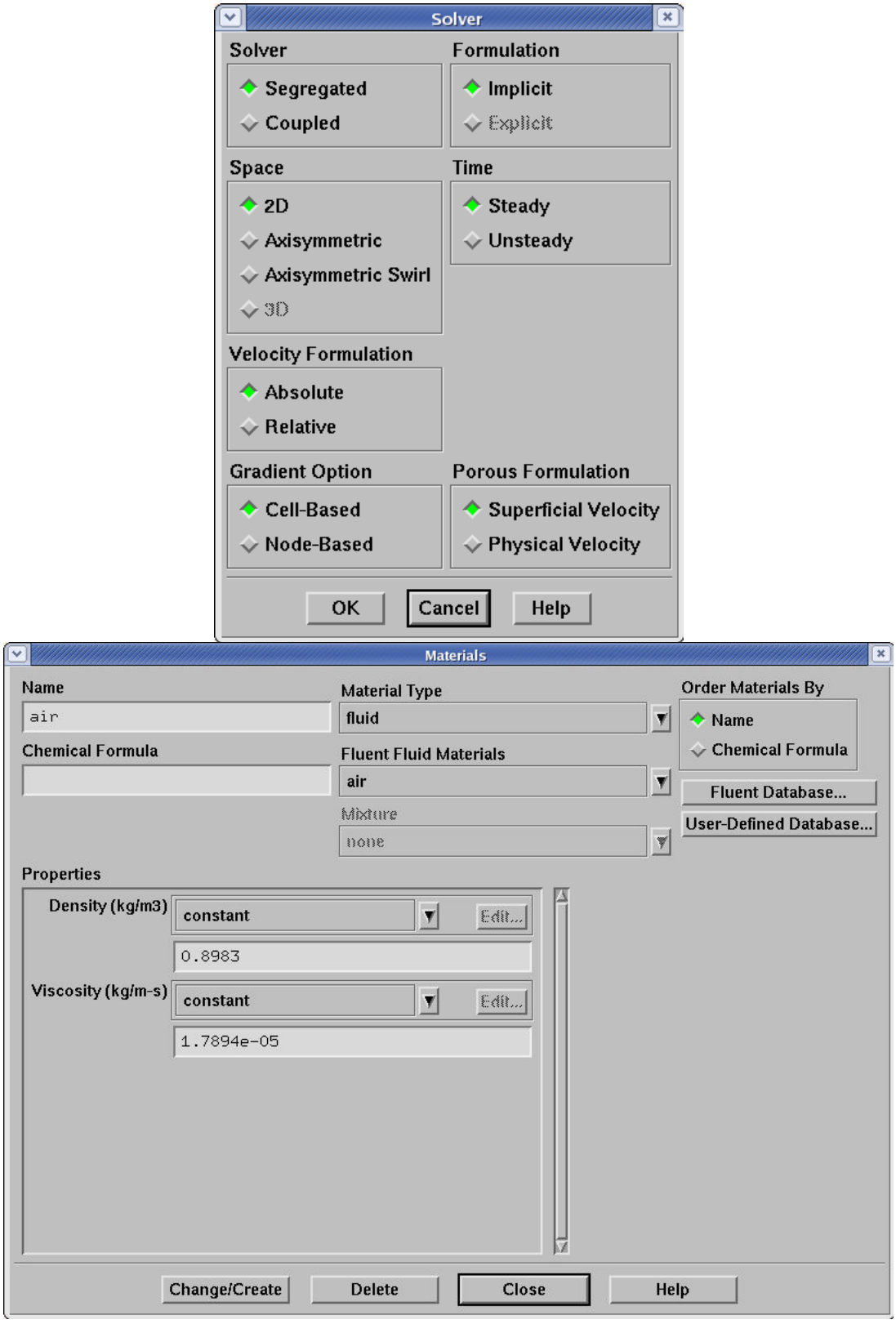
Solver
Solver
Segregated
Coupled
Formulation
Implicit
Explicit
Space
2D
Axisymmetric
Axisymmetric Swirl
3D
Time
Steady
Unsteady
Velocity Formulation
Absolute
Relative
Gradient Option
Cell-Based
Node-Based
Porous Formulation
Superficial Velocity
Physical Velocity
OK
Cancel
Help
Materials
Name
air
Material Type
fluid
Order Materials By
Name
Chemical Formula
Chemical Formula
Fluent Fluid Materials
air
Fluent Database...
Mixture
none
User-Defined Database...
Properties
Density (kg/m3)
constant
Edit...
0.8983
Viscosity (kg/m-s)
constant
Edit...
1.7894e-05
Change/Create
Delete
Close
Help

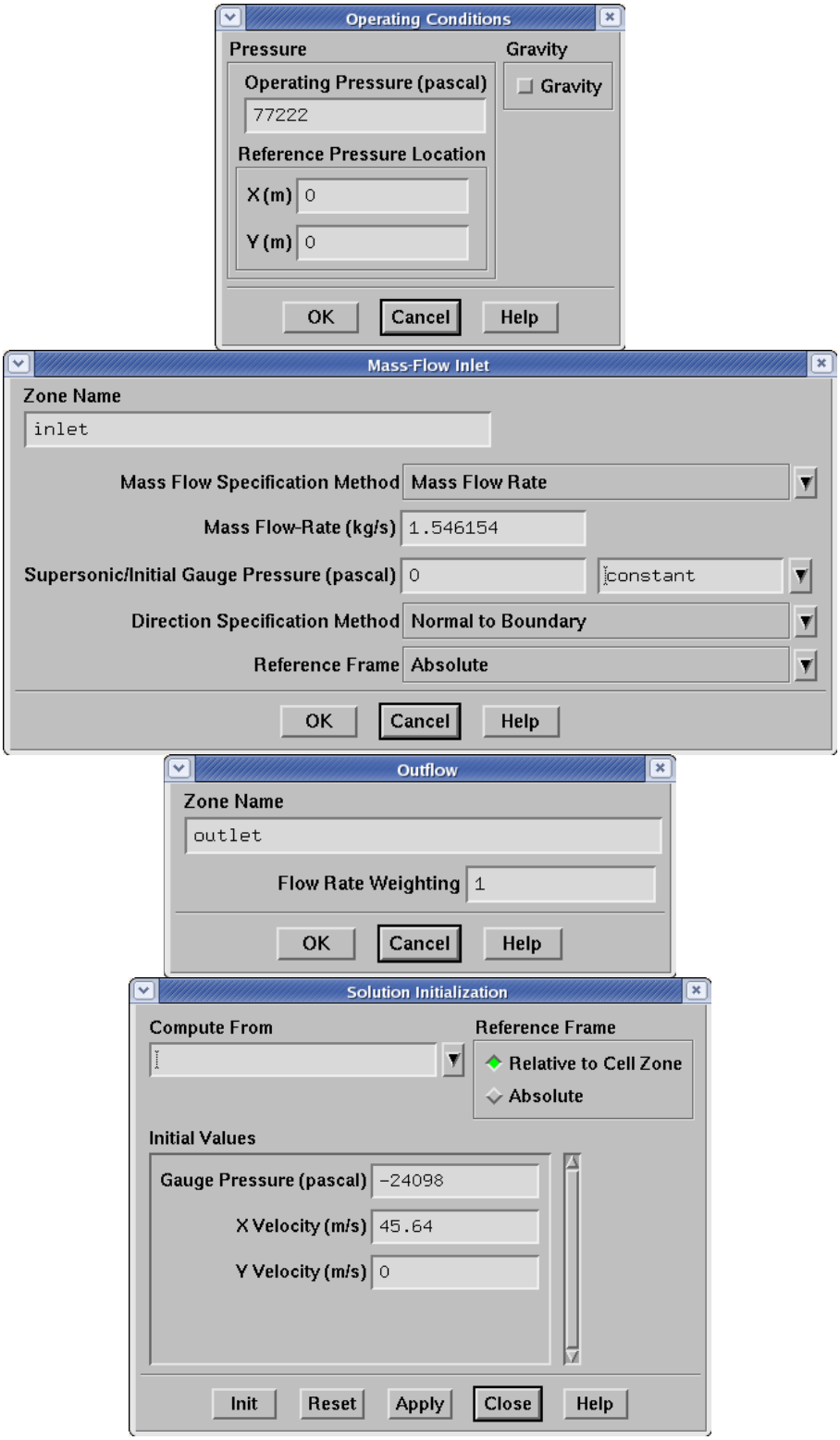
Operating Conditions
Pressure
Operating Pressure (pascal)
77222
Reference Pressure Location
X (m) 0
Y (m) 0
Gravity
Gravity
OK
Cancel
Help
Mass-Flow Inlet
Zone Name
inlet
Mass Flow Specification Method
Mass Flow Rate
Mass Flow Rate (kg/s) 1.546154
Supersonic/Initial Gauge Pressure (pascal) 0
constant
Direction Specification Method
Normal to Boundary
Reference Frame
Absolute
OK
Cancel
Help
Outflow
Zone Name
outlet
Flow Rate Weighting 1
OK
Cancel
Help
Solution Initialization
Compute From
Reference Frame
Relative to Cell Zone
Absolute
Initial Values
Gauge Pressure (pascal) -24098
X Velocity (m/s) 45.64
Y Velocity (m/s) 0
Init
Reset
Apply
Close
Help

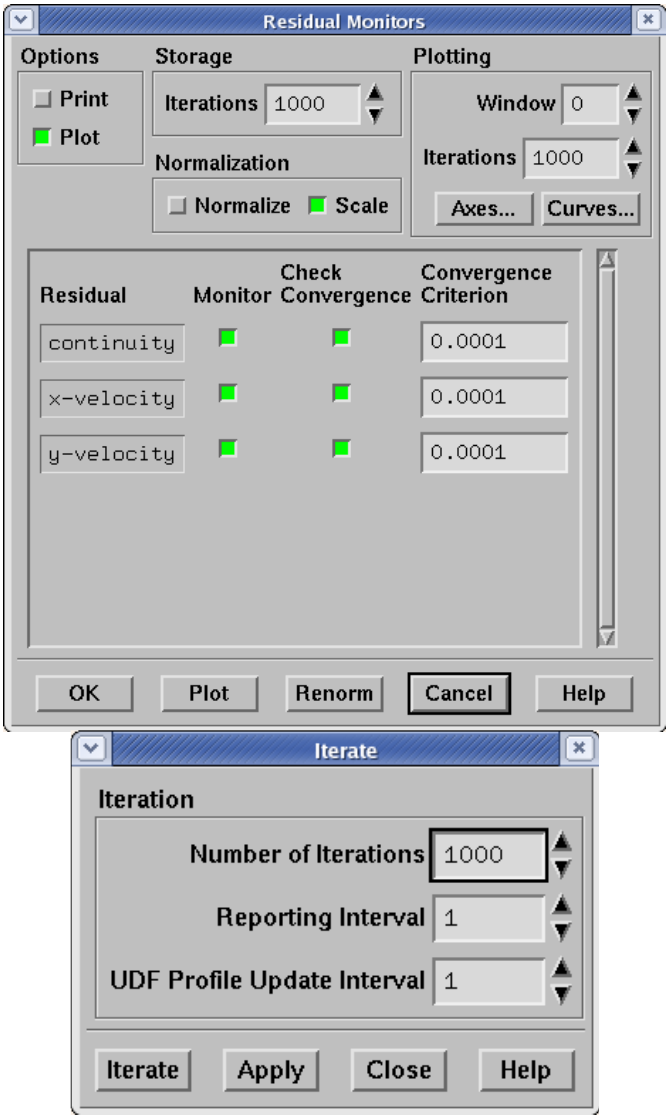
Residual Monitors
Options
Print
Plot
Storage
Iterations 1000
Normalization
Normalize
Scale
Plotting
Window 0
Iterations 1000
Axes...
Curves...
Residual
Monitor
Check Convergence
Convergence Criterion
continuity
0.0001
x-velocity
0.0001
y-velocity
0.0001
OK
Plot
Renorm
Cancel
Help
Iterate
Iteration
Number of Iterations 1000
Reporting Interval 1
UDF Profile Update Interval 1
Iterate
Apply
Close
Help

Appendix C: Data Tables

Particle Trajectories In Engine With Different Initial Particle Velocities

Engine Model		Engine Model		Engine Model	
Initial Velocity = 100ft/s		Initial Velocity = 300ft/s		Initial Velocity = 500ft/s	
Total Deflection (inches)	0.009640916	Total Deflection (inches)	0.001148936	Total Deflection (inches)	0.000425035
X	Y	X	Y	X	Y
0.011999978	0.984250002	0.03599993	0.984250002	0.059999882	0.984250002
0.024000382	0.984250005	0.071998421	0.984250005	0.119987001	0.984250005
0.036001639	0.984250008	0.107994036	0.984250008	0.179948618	0.984250008
0.048003747	0.984250011	0.143986777	0.984250011	0.239884787	0.984250011
0.060006707	0.984250014	0.17997665	0.984250014	0.299795564	0.984250014
0.072010519	0.984250017	0.21596366	0.984250017	0.359681011	0.984250017
0.084015182	0.98425002	0.251947812	0.98425002	0.419541188	0.98425002
0.096020698	0.984250023	0.287929112	0.984250023	0.479376158	0.984250023
0.108027066	0.984250026	0.323907566	0.984250026	0.539185991	0.984250026
0.120034287	0.984250029	0.35988318	0.984250029	0.598970756	0.984250029
0.132042361	0.984250032	0.395855962	0.984250032	0.658730529	0.984250032
0.144051287	0.984250035	0.431825917	0.984250035	0.718465388	0.984250035
0.156061067	0.984250038	0.467793055	0.984250038	0.778175418	0.984250038
0.1680717	0.984250041	0.503757382	0.984250041	0.837860709	0.984250041
0.180083187	0.984250044	0.539718907	0.984250044	0.897521359	0.984250045
0.192095528	0.984250047	0.57567764	0.984250047	0.95715747	0.984250049
0.204108723	0.98425005	0.611633588	0.98425005	1.016769155	0.984250053
0.216122773	0.984250053	0.647586762	0.984250053	1.076356534	0.984250057
0.228137678	0.984250056	0.683537173	0.984250056	1.135919745	0.984250062
0.240153438	0.984250059	0.719484831	0.984250059	1.195458936	0.984250068
0.252170053	0.984250062	0.755429749	0.984250063	1.254974259	0.984250074
0.264187525	0.984250065	0.791371938	0.984250066	1.31446588	0.984250082
0.276205853	0.984250068	0.827311412	0.98425007	1.373933978	0.984250091
0.288225038	0.984250071	0.863248185	0.984250073	1.433378747	0.984250101
0.300245079	0.984250074	0.899182273	0.984250077	1.4928004	0.984250113
0.312265978	0.984250077	0.93511369	0.984250081	1.552199169	0.984250128
0.324287735	0.98425008	0.971042455	0.984250086	1.611575307	0.984250145
0.33631035	0.984250083	1.006968585	0.984250091	1.670929097	0.984250167
0.348333823	0.984250086	1.042892099	0.984250096	1.730260847	0.984250193
0.360358155	0.984250089	1.078813018	0.984250102	1.789570904	0.984250225
0.372383347	0.984250092	1.114731364	0.984250108	1.848859654	0.984250264
0.384409399	0.984250095	1.15064716	0.984250115	1.90812752	0.984250315
0.396436311	0.984250099	1.186560426	0.984250123	1.967374964	0.984250381
0.408464084	0.984250102	1.222471191	0.984250131	2.026602452	0.984250469
0.420492717	0.984250105	1.258379482	0.984250141	2.085810426	0.98425059
0.432522213	0.984250108	1.294285325	0.984250151	2.144999314	0.984250755
0.444552571	0.984250111	1.330188748	0.984250163	2.204169464	0.98425098
0.456583792	0.984250114	1.366089785	0.984250176	2.263321285	0.984251292
0.468615875	0.984250117	1.401988471	0.984250191	2.322455242	0.984251725
0.480648823	0.98425012	1.437884839	0.984250208	2.381571505	0.984252329
0.492682635	0.984250123	1.473778924	0.984250226	2.440670061	0.984253174
0.504717312	0.984250126	1.509670768	0.984250247	2.49975073	0.984254324
0.516752854	0.984250129	1.545560414	0.98425027	2.558812988	0.984255838

0.528789263	0.984250132	1.581447905	0.984250296	2.617856314	0.984257781
0.540826539	0.984250135	1.617333284	0.984250326	2.676880282	0.984260224
0.552864682	0.984250138	1.653216605	0.98425036	2.735884311	0.984263253
0.564903693	0.984250141	1.689097923	0.984250398	2.794867756	0.984266945
0.576943573	0.984250144	1.724977292	0.984250442	2.853829908	0.984271374
0.588984322	0.984250147	1.760854767	0.984250491	2.912769928	0.984276623
0.601025942	0.98425015	1.796730408	0.984250548	2.971686906	0.984282772
0.613068433	0.984250153	1.832604287	0.984250613	3.030579803	0.984289888
0.625111795	0.984250157	1.868476479	0.984250688	3.089447672	0.984298021
0.63715603	0.98425016	1.904347051	0.984250776	3.148289462	0.984307216
0.649201139	0.984250163	1.940216085	0.98425088	3.207103908	0.984317532
0.661247122	0.984250166	1.976083659	0.984251005	3.265889842	0.984329006
0.67329398	0.98425017	2.011949839	0.984251154	3.324646047	0.98434165
0.685341714	0.984250173	2.047814688	0.984251335	3.383371214	0.984355503
0.697390325	0.984250177	2.083678272	0.984251555	3.442063956	0.98437058
0.709439814	0.98425018	2.119540658	0.984251822	3.500722811	0.984386896
0.721490181	0.984250184	2.155401889	0.984252147	3.559346167	0.984404469
0.733541429	0.984250188	2.191262013	0.984252543	3.617932664	0.984423296
0.745593557	0.984250191	2.227121092	0.984253023	3.676480871	0.984443379
0.757646567	0.984250195	2.26297919	0.984253606	3.734989009	0.984464718
0.76970046	0.9842502	2.298836363	0.984254314	3.79345545	0.984487284
0.781755238	0.984250204	2.33469266	0.984255183	3.851878269	0.984511051
0.793810901	0.984250208	2.370548078	0.984256249	3.910255451	0.984535986
0.805867451	0.984250213	2.406402587	0.984257551	3.968585185	0.984562019
0.817924888	0.984250217	2.442256148	0.98425913	4.026865131	0.984589105
0.829983215	0.984250222	2.478108712	0.984261023	4.085092624	0.984617147
0.842042431	0.984250227	2.513960226	0.98426327	4.143265377	0.984645892
0.854102539	0.984250233	2.549810601	0.984265914	4.201380707	0.984675037
0.86616354	0.984250238	2.585659784	0.984268993		
0.878225435	0.984250244	2.621507717	0.984272549		
0.890288227	0.98425025	2.657354301	0.984276624		
0.902351915	0.984250256	2.693199444	0.984281274		
0.914416503	0.984250263	2.729043039	0.984286551		
0.926481991	0.98425027	2.764884937	0.984292498		
0.93854838	0.984250277	2.800725021	0.984299166		
0.950615672	0.984250284	2.836563157	0.984306602		
0.96268387	0.984250292	2.872399147	0.984314849		
0.974752974	0.9842503	2.908232845	0.984323946		
0.986822987	0.984250309	2.944064095	0.984333935		
0.998893911	0.984250318	2.979892672	0.984344857		
1.010965746	0.984250327	3.015718343	0.984356754		
1.023038495	0.984250337	3.051540877	0.984369659		
1.035112159	0.984250348	3.087360028	0.984383602		
1.047186741	0.984250358	3.123175523	0.984398611		
1.059262243	0.98425037	3.158987076	0.984414713		
1.071338667	0.984250382	3.194794395	0.984431936		
1.083416014	0.984250394	3.230597153	0.984450303		
1.095494288	0.984250407	3.266395036	0.98446984		
1.107573489	0.984250421	3.302187772	0.984490569		
1.11965362	0.984250435	3.337975024	0.98451249		

1.131734684	0.98425045
1.143816683	0.984250466
1.15589962	0.984250483
1.167983497	0.9842505
1.180068315	0.984250518
1.192154079	0.984250537
1.204240789	0.984250557
1.21632845	0.984250577
1.228417064	0.984250599
1.240506635	0.984250622
1.252597164	0.984250646
1.264688655	0.984250671
1.27678111	0.984250697
1.288874532	0.984250724
1.300968926	0.984250753
1.313064295	0.984250782
1.325160641	0.984250813
1.337257969	0.984250846
1.349356281	0.98425088
1.361455581	0.984250915
1.373555872	0.984250953
1.38565716	0.984250991
1.397759447	0.984251032
1.409862738	0.984251074
1.421967038	0.984251118
1.434072348	0.984251164
1.446178675	0.984251212
1.458286021	0.984251262
1.470394393	0.984251315
1.482503795	0.98425137
1.494614231	0.984251427
1.506725708	0.984251487
1.518838228	0.98425155
1.530951798	0.984251615
1.543066421	0.984251683
1.555182105	0.984251755
1.567298856	0.984251829
1.579416678	0.984251907
1.591535579	0.984251989
1.603655562	0.984252074
1.615776635	0.984252163
1.627898803	0.984252256
1.640022075	0.984252353
1.652146456	0.984252455
1.664271955	0.984252561
1.676398579	0.984252673
1.688526333	0.984252789
1.700655225	0.984252912
1.712785266	0.984253039
1.724916466	0.984253173
3.373756396	0.984535613
3.409531535	0.984559964
3.445300065	0.984585574
3.481061588	0.984612446
3.516815713	0.984640574
3.552562028	0.984669953
3.588300092	0.984700583
3.624029451	0.984732469
3.659749638	0.984765613
3.695460159	0.984800018
3.731160516	0.984835688
3.766850115	0.984872592
3.802528317	0.984910697
3.838194526	0.984949998
3.873848101	0.984990493
3.909488443	0.98503216
3.945115032	0.985074965
3.980726892	0.985118846
4.016322996	0.985163724
4.05190271	0.985209514
4.087465089	0.985256093
4.123009235	0.985303304
4.158534852	0.985350969
4.19404097	0.985398938

1.737048829	0.984253314
1.749182365	0.984253461
1.761317083	0.984253616
1.773452994	0.984253778
1.785590107	0.984253948
1.797728431	0.984254127
1.809867979	0.984254315
1.822008757	0.984254512
1.834150776	0.98425472
1.846294048	0.984254939
1.858438584	0.984255169
1.870584397	0.984255412
1.882731498	0.984255669
1.894879901	0.984255941
1.907029613	0.984256229
1.919180648	0.984256534
1.931333017	0.984256858
1.943486735	0.984257202
1.955641813	0.984257568
1.96779826	0.984257958
1.979956089	0.984258372
1.992115315	0.984258816
2.004275951	0.984259289
2.016438005	0.984259795
2.028601488	0.984260335
2.040766412	0.984260912
2.052932784	0.984261527
2.065100613	0.984262184
2.077269917	0.984262886
2.089440695	0.984263637
2.101612947	0.984264441
2.11378669	0.984265302
2.125961934	0.984266222
2.138138687	0.984267204
2.150316969	0.984268254
2.162496795	0.984269376
2.174678175	0.984270573
2.186861124	0.98427185
2.199045664	0.984273215
2.21123181	0.984274674
2.223419572	0.984276233
2.235608967	0.984277899
2.24780001	0.984279681
2.259992714	0.984281589
2.272187093	0.984283632
2.284383158	0.984285818
2.296580918	0.98428816
2.308780388	0.984290673
2.320981546	0.98429337
2.33318437	0.984296262

2.345388864	0.984299364
2.357595029	0.984302685
2.369802865	0.984306242
2.382012373	0.984310049
2.394223549	0.984314123
2.406436366	0.984318474
2.418650796	0.984323112
2.430866835	0.984328054
2.443084476	0.984333315
2.455303717	0.984338905
2.46752453	0.984344833
2.479746889	0.984351116
2.491970787	0.984357767
2.50419622	0.984364798
2.516423164	0.984372218
2.528651591	0.984380051
2.540881494	0.984388312
2.553112869	0.984397015
2.565345695	0.984406169
2.577579947	0.984415792
2.589815619	0.984425903
2.602052705	0.984436513
2.614291202	0.984447635
2.626531081	0.984459288
2.638772314	0.984471489
2.651014895	0.98448425
2.663258816	0.984497585
2.675504064	0.984511516
2.687750602	0.984526064
2.699998402	0.984541241
2.712247454	0.984557062
2.724497747	0.984573548
2.736749264	0.984590724
2.749001978	0.984608601
2.761255861	0.984627187
2.773510897	0.984646508
2.785767076	0.984666579
2.798024369	0.984687409
2.810282745	0.984709007
2.822542187	0.984731398
2.834802683	0.984754598
2.847064204	0.984778613
2.859326714	0.984803461
2.8715902	0.984829158
2.883854653	0.984855719
2.896120036	0.98488316
2.908386316	0.984911498
2.920653482	0.98494075
2.932921507	0.984970923
2.945190366	0.985002026

2.957460046	0.985034076
2.969730537	0.985067089
2.982001807	0.985101084
2.994273832	0.985136066
3.006546605	0.985172045
3.018820095	0.985209036
3.031094272	0.985247057
3.04336913	0.985286115
3.055644643	0.985326217
3.067920782	0.985367377
3.080197538	0.985409603
3.092474888	0.9854529
3.104752798	0.985497279
3.117031263	0.98554275
3.129310261	0.985589318
3.14158977	0.985636989
3.153869784	0.985685772
3.166150284	0.985735693
3.178431249	0.985786758
3.190712661	0.98583896
3.202994501	0.985892325
3.215276747	0.985946853
3.227559381	0.986002531
3.23984239	0.986059376
3.252125764	0.986117402
3.264409476	0.986176612
3.276693508	0.986237004
3.288977854	0.986298584
3.301262496	0.986361374
3.313547418	0.986425372
3.325832607	0.986490566
3.338118055	0.986556971
3.35040375	0.986624605
3.362689676	0.986693462
3.374975816	0.986763542
3.387262163	0.986834859
3.399548705	0.986907403
3.411835427	0.986981171
3.424122315	0.987056188
3.436409359	0.987132441
3.448696545	0.987209928
3.460983865	0.987288666
3.473271314	0.987368662
3.485558882	0.987449905
3.497846555	0.987532392
3.510134322	0.987616151
3.522422175	0.987701171
3.534710104	0.987787444
3.546998107	0.987874979
3.559286175	0.987963766

3.571574298	0.988053805
3.58386247	0.988145118
3.596150686	0.988237696
3.608438939	0.988331533
3.620727223	0.988426619
3.633015531	0.988522942
3.645303862	0.988620513
3.657592209	0.988719333
3.669880567	0.988819405
3.682168933	0.988920739
3.694457306	0.989023328
3.706745682	0.989127163
3.719034059	0.989232234
3.731322436	0.989338526
3.743610803	0.98944603
3.755899137	0.989554745
3.768187421	0.989664694
3.780475611	0.989775863
3.792763666	0.989888243
3.805051562	0.990001843
3.817339234	0.990116651
3.829626608	0.990232653
3.841913596	0.990349837
3.854200099	0.990468187
3.86648607	0.990587713
3.878771383	0.990708401
3.891055863	0.990830245
3.90333929	0.990953239
3.915621496	0.991077363
3.927902378	0.991202628
3.940181731	0.99132901
3.952459322	0.991456483
3.96473491	0.991585018
3.977008215	0.991714582
3.989278965	0.991845137
4.001546834	0.991976642
4.013811594	0.992109099
4.026073177	0.992242457
4.038331222	0.992376663
4.050585423	0.992511655
4.062835421	0.992647364
4.075080874	0.992783777
4.087321471	0.992920811
4.099556903	0.993058384
4.111787134	0.993196403
4.124011421	0.993334752
4.136229067	0.993473409
4.148439597	0.993612339
4.160642538	0.993751509
4.172837904	0.993890918

Particle Trajectories In Rig With Different Particle Diameters

Engine Model		Engine Model		Engine Model	
Diameter = .005 inches		Diameter = .02 inches		Diameter = .1 inches	
Total Deflection (inches)	0.033506147	Total Deflection (inches)	0.003852748	Total Deflection (inches)	0.00062806
X	Y	X	Y	X	Y
0.033464567	0.984250067	0.033464506	0.98425	0.033464501	0.984250001
0.06688937	0.984250201	0.066925157	0.98425	0.066928693	0.984250002
0.100235213	0.984250335	0.100378094	0.984250039	0.100392269	0.984250003
0.133503476	0.984250469	0.133823338	0.984250039	0.133855228	0.984250004
0.166695534	0.984250603	0.167260913	0.984250039	0.167317573	0.984250005
0.199812743	0.984250737	0.200690841	0.984250079	0.200779303	0.984250006
0.232856414	0.984250871	0.234113149	0.984250079	0.23424042	0.984250007
0.265827846	0.984251005	0.267527862	0.984250079	0.267700926	0.984250008
0.298728332	0.984251139	0.300935006	0.984250118	0.301160821	0.984250009
0.331559139	0.984251273	0.334334608	0.984250118	0.334620106	0.98425001
0.364321488	0.984251407	0.367726699	0.984250118	0.368078784	0.984250011
0.397016576	0.984251541	0.401111306	0.984250157	0.401536856	0.984250012
0.429645601	0.984251675	0.434488456	0.984250157	0.434994322	0.984250013
0.462209742	0.984251809	0.467858181	0.984250157	0.468451185	0.984250014
0.494710158	0.984251943	0.501220512	0.984250197	0.501907447	0.984250015
0.527147971	0.984252077	0.534575484	0.984250197	0.535363108	0.984250016
0.559524283	0.984252211	0.567923131	0.984250197	0.568818172	0.984250017
0.591840212	0.984252346	0.601263489	0.984250236	0.602272639	0.984250018
0.624096867	0.984252483	0.634596595	0.984250236	0.635726513	0.984250019
0.656295344	0.984252622	0.66792249	0.984250236	0.669179796	0.98425002
0.688436733	0.984252766	0.701241214	0.984250276	0.702632489	0.984250021
0.720522118	0.984252915	0.734552811	0.984250276	0.736084597	0.984250022
0.752552534	0.984253071	0.767857326	0.984250315	0.769536121	0.984250024
0.784529013	0.984253234	0.801154805	0.984250315	0.802987065	0.984250025
0.816452619	0.984253407	0.834445299	0.984250315	0.836437432	0.984250026
0.848324416	0.984253591	0.867728859	0.984250354	0.869887225	0.984250027
0.880145413	0.984253788	0.90100554	0.984250354	0.903336448	0.984250029
0.911916622	0.984253999	0.934275398	0.984250394	0.936785105	0.98425003
0.943639097	0.984254227	0.967538493	0.984250394	0.970233199	0.984250032
0.975313896	0.984254473	1.000794887	0.984250433	1.003680736	0.984250033
1.006942078	0.984254742	1.034044639	0.984250433	1.03712772	0.984250035
1.038524643	0.984255034	1.067287809	0.984250472	1.070574155	0.984250037
1.070062593	0.984255353	1.100524467	0.984250512	1.104020047	0.984250039
1.101556993	0.984255703	1.133754687	0.984250551	1.137465401	0.984250041
1.133008846	0.984256086	1.166978548	0.984250591	1.170910223	0.984250044
1.164419156	0.984256505	1.200196129	0.98425063	1.204354519	0.984250047
1.195789004	0.984256966	1.233407515	0.984250669	1.237798295	0.98425005
1.227119479	0.984257472	1.266612796	0.984250709	1.271241558	0.984250053
1.258411598	0.984258028	1.299812064	0.984250748	1.304684315	0.984250057
1.289666385	0.984258639	1.333005415	0.984250827	1.338126572	0.984250061
1.320884955	0.98425931	1.366192952	0.984250866	1.371568337	0.984250066
1.352068344	0.984260047	1.39937478	0.984250945	1.405009616	0.984250071
1.383217598	0.984260855	1.432551012	0.984251024	1.43845042	0.984250077
1.41433387	0.984261743	1.465721764	0.984251102	1.471890757	0.984250084

1.445418331	0.98426272	1.498887159	0.98425122	1.505330636	0.984250091
1.47647206	0.984263793	1.532047325	0.984251339	1.538770068	0.984250099
1.507496153	0.984264972	1.565202397	0.984251457	1.572209064	0.984250108
1.538491834	0.98426627	1.598352499	0.984251575	1.605647634	0.984250119
1.569460227	0.984267697	1.631497762	0.984251732	1.63908579	0.98425013
1.600402472	0.984269267	1.664638341	0.98425189	1.672523545	0.984250143
1.631319863	0.984270996	1.697774397	0.984252087	1.705960913	0.984250158
1.66221358	0.984272902	1.730906102	0.984252283	1.739397906	0.984250175
1.693084827	0.984275004	1.764033635	0.98425252	1.772834541	0.984250194
1.723934822	0.984277322	1.797157185	0.984252795	1.806270832	0.984250216
1.75476481	0.984279883	1.830276949	0.98425311	1.839706795	0.984250241
1.78557621	0.98428272	1.863393131	0.984253425	1.873142449	0.984250271
1.816370472	0.984285878	1.896505942	0.984253819	1.906577809	0.984250305
1.847148891	0.984289404	1.929615593	0.984254291	1.940012894	0.984250346
1.877912767	0.984293358	1.962722294	0.984254803	1.973447722	0.984250395
1.908663386	0.984297809	1.995826221	0.984255433	2.006882305	0.984250454
1.939401997	0.984302843	2.028927535	0.984256181	2.040316658	0.984250524
1.970129948	0.984308578	2.062026409	0.984257008	2.073750795	0.984250608
2.000848334	0.984315138	2.095122949	0.984258031	2.107184729	0.984250711
2.031558136	0.984322661	2.128217255	0.984259213	2.140618471	0.984250835
2.062260374	0.984331316	2.161309493	0.984260591	2.174052032	0.984250986
2.092956002	0.984341287	2.194399834	0.984262205	2.207485426	0.98425117
2.123645492	0.984352764	2.227488448	0.984264134	2.240918668	0.984251393
2.154329304	0.984365964	2.260575501	0.984266417	2.27435177	0.984251665
2.185008339	0.984381165	2.29366114	0.984269134	2.307784745	0.984251996
2.215683356	0.98439867	2.326745471	0.984272362	2.34121759	0.9842524
2.246355045	0.984418831	2.359828478	0.984276142	2.374650305	0.984252896
2.277024029	0.984442053	2.392910114	0.984280709	2.408082891	0.984253501
2.307690805	0.984468834	2.425990287	0.984286063	2.441515339	0.984254234
2.338355389	0.984499803	2.459068881	0.984292401	2.474947638	0.984255112
2.369017631	0.984535656	2.492145766	0.984299764	2.508379776	0.984256155
2.399677607	0.984577064	2.525220812	0.984308268	2.541811734	0.984257378
2.430334879	0.984624614	2.558293874	0.984318031	2.575243499	0.984258802
2.460988904	0.984678977	2.591364714	0.984329094	2.608675057	0.984260447
2.491639105	0.984740702	2.624433154	0.984341653	2.642106385	0.984262332
2.522284897	0.984810227	2.657498987	0.984355827	2.675537464	0.984264483
2.552925556	0.984888169	2.690561976	0.984371771	2.708968267	0.984266924
2.583560338	0.984975149	2.72362183	0.984389527	2.742398769	0.98426968
2.614188425	0.985071701	2.756678233	0.98440933	2.775828944	0.984272771
2.644808262	0.985178431	2.789730878	0.98443122	2.80925876	0.984276222
2.675418627	0.985295976	2.822779311	0.984455275	2.842688181	0.984280058
2.70601786	0.985424995	2.855823135	0.984481614	2.876117162	0.984284293
2.736604352	0.985566102	2.888861862	0.984510393	2.909545655	0.984288938
2.767176436	0.985719808	2.921894806	0.984541732	2.942973612	0.984294019
2.797732067	0.98588676	2.954921305	0.984575669	2.976400987	0.98429956
2.828268596	0.986067711	2.987940843	0.984612322	3.009827721	0.98430558
2.858783118	0.986263412	3.020952863	0.98465181	3.043253748	0.984312094
2.889272978	0.986474336	3.053956598	0.984694251	3.076679	0.984319119
2.919734178	0.986700819	3.086951299	0.984739645	3.1101034	0.98432667
2.950163329	0.986943465	3.11993613	0.98478807	3.143526881	0.984334765

2.98055693	0.98720289
3.010910566	0.987479434
3.041219469	0.987773424
3.071479419	0.988085467
3.101686407	0.988416009
3.13183503	0.988765147
3.161919003	0.989133114
3.191932228	0.989520156
3.221869297	0.989926675
3.251724335	0.990352966
3.281490989	0.990799266
3.311162933	0.991265805
3.340732307	0.991752563
3.370193849	0.992259669
3.39954206	0.992787259
3.428768493	0.993335334
3.457866181	0.993904177
3.486829023	0.994493934
3.515650251	0.995104351
3.544322826	0.99573521
3.572840448	0.996386766
3.601196442	0.997059269
3.629383127	0.997752583
3.657392658	0.998466565
3.685218337	0.999200896
3.712850074	0.999955611
3.740281416	1.000731021
3.767508974	1.001527062
3.794525435	1.002343365
3.821321606	1.003179746
3.847888031	1.004035994
3.874216902	1.00491168
3.900300072	1.005806319
3.926128996	1.00671935
3.95169573	1.007650819
3.976991021	1.008600685
4.002002915	1.009568061
4.026718324	1.010551792
4.051123217	1.011550353
4.075204432	1.012562787
4.098947797	1.013587661
4.122339805	1.014622108
4.145380068	1.015662789
4.168079433	1.016707881
4.1904093	1.017756214
3.152910129	0.984839605
3.185872302	0.984894329
3.218821881	0.984952321
3.25175809	0.985013581
3.284679623	0.985078187
3.317585411	0.98514614
3.350474594	0.985217557
3.383345889	0.98529236
3.416198031	0.985370549
3.449029907	0.985452281
3.48184034	0.985537517
3.514627957	0.985626257
3.547391289	0.985718501
3.580128779	0.985814249
3.612838812	0.98591354
3.645519975	0.986016296
3.678170711	0.986122516
3.710789278	0.98623224
3.74337411	0.98634539
3.775923439	0.986462003
3.808435217	0.986582003
3.840907633	0.986705428
3.873338645	0.98683216
3.90572611	0.986962199
3.938067805	0.987095427
3.970360679	0.987231884
4.00260181	0.987371332
4.034788732	0.987513655
4.066918843	0.987658458
4.098989914	0.98780515
4.13100072	0.987953339
4.162950104	0.988102748
3.176949394	0.984343418
3.210370867	0.984352633
3.243791201	0.98436242
3.277210316	0.98437279
3.31062813	0.984383752
3.344044529	0.984395312
3.37745941	0.98440747
3.410872685	0.984420238
3.44428424	0.984433631
3.477693955	0.98444765
3.511101712	0.984462292
3.544507385	0.984477555
3.577910839	0.984493439
3.611311934	0.984509947
3.644710548	0.984527074
3.678106544	0.984544817
3.71149977	0.984563178
3.744890089	0.984582152
3.778277344	0.984601732
3.811661357	0.984621919
3.845041934	0.984642711
3.878418895	0.9846641
3.911792082	0.98468607
3.945161288	0.984708587
3.978526205	0.984731618
4.011886546	0.98475514
4.045242106	0.984779109
4.078592686	0.98480347
4.111937996	0.984828142
4.145277834	0.984853031
4.178611885	0.984878061

Particle Trajectories In Engine With Different Initial Distances from Bleed Wall

Engine Model		Engine Model		Engine Model	
Initial Position = .7243 in. from wall		Initial Position = .3306 in. from wall		Initial Position = .118 in. from wall	
Total Deflection (inches)	0.000210274	Total Deflection (inches)	0.000796738	Total Deflection (inches)	0.001542548
X	Y	X	Y	X	Y
0.033464502	0.393700002	0.033464502	0.787400002	0.033464502	1.062990002
0.066928103	0.393700005	0.066928103	0.787400005	0.066928104	1.062990005
0.100389902	0.393700008	0.100389903	0.787400008	0.100389912	1.062990008
0.1338499	0.393700011	0.133849902	0.787400011	0.133849929	1.062990011
0.167308096	0.393700014	0.167308103	0.787400014	0.167308163	1.062990014
0.20076449	0.393700017	0.200764506	0.787400017	0.200764616	1.062990017
0.234219085	0.393700021	0.234219114	0.78740002	0.234219294	1.06299002
0.267671879	0.393700024	0.267671931	0.787400023	0.267672201	1.062990023
0.301122872	0.393700028	0.301122957	0.787400026	0.301123341	1.062990026
0.334572066	0.393700032	0.334572198	0.78740003	0.334572719	1.062990029
0.36801946	0.393700036	0.368019656	0.787400033	0.36802034	1.062990032
0.401465054	0.393700041	0.401465334	0.787400037	0.401466207	1.062990035
0.434908849	0.393700046	0.434909238	0.787400041	0.434910326	1.062990038
0.468350845	0.393700052	0.468351369	0.787400045	0.468352702	1.062990041
0.50179104	0.393700058	0.501791732	0.787400049	0.501793341	1.062990044
0.535229434	0.393700065	0.535230332	0.787400053	0.535232249	1.062990047
0.568666029	0.393700072	0.568667174	0.787400058	0.568669433	1.06299005
0.602100822	0.393700081	0.602102263	0.787400063	0.602104898	1.062990053
0.635533816	0.393700091	0.635535603	0.787400069	0.635538652	1.062990056
0.668965008	0.393700102	0.668967203	0.787400075	0.668970702	1.062990059
0.702394401	0.393700114	0.702397068	0.787400082	0.702401057	1.062990062
0.735821994	0.393700128	0.735825206	0.78740009	0.735829724	1.062990065
0.76924779	0.393700144	0.769251624	0.787400099	0.769256712	1.062990068
0.802671789	0.393700163	0.80267633	0.787400108	0.802682032	1.062990071
0.836093996	0.393700184	0.836099331	0.787400118	0.836105692	1.062990074
0.869514415	0.393700209	0.869520638	0.78740013	0.869527704	1.062990077
0.902933048	0.393700237	0.902940261	0.787400143	0.902948079	1.06299008
0.936349902	0.393700269	0.936358208	0.787400157	0.936366828	1.062990083
0.969764983	0.393700306	0.969774491	0.787400173	0.969783965	1.062990086
1.003178299	0.393700348	1.003189121	0.787400191	1.003199501	1.062990089
1.036589858	0.393700396	1.03660211	0.787400211	1.036613452	1.062990092
1.069999667	0.393700449	1.070013471	0.787400234	1.070025831	1.062990096
1.103407738	0.39370051	1.103423217	0.787400259	1.103436656	1.062990099
1.13681408	0.393700578	1.136831363	0.787400287	1.136845941	1.062990102
1.170218706	0.393700654	1.170237922	0.787400318	1.170253704	1.062990105
1.203621626	0.393700739	1.203642911	0.787400352	1.203659961	1.062990108
1.237022845	0.393700833	1.237046346	0.78740039	1.23706473	1.062990112
1.270422367	0.393700938	1.270448243	0.787400433	1.270468029	1.062990115
1.303820202	0.393701054	1.303848621	0.78740048	1.30386988	1.062990119
1.337216362	0.393701182	1.337247496	0.787400533	1.337270305	1.062990123
1.370610857	0.393701324	1.370644884	0.787400591	1.370669328	1.062990127
1.404003697	0.393701479	1.404040807	0.787400655	1.404066974	1.062990132
1.437394891	0.393701651	1.437435284	0.787400726	1.437463268	1.062990136
1.470784445	0.393701838	1.470828338	0.787400804	1.470858238	1.062990142

1.50417237	0.393702044	1.504219991	0.787400891	1.504251913	1.062990147
1.537558675	0.393702269	1.537610266	0.787400987	1.537644325	1.062990154
1.570943367	0.393702515	1.570999187	0.787401093	1.571035505	1.062990161
1.604326454	0.393702784	1.60438678	0.78740121	1.604425488	1.062990168
1.637707949	0.393703078	1.63777307	0.78740134	1.637814311	1.062990177
1.671087848	0.3937034	1.671158084	0.787401484	1.671202013	1.062990187
1.704466149	0.393703752	1.70454185	0.787401643	1.704588635	1.062990198
1.737842859	0.393704137	1.737924395	0.787401821	1.737974221	1.062990211
1.771217986	0.393704556	1.771305744	0.787402019	1.771358819	1.062990225
1.804591537	0.393705014	1.804685924	0.787402239	1.804742481	1.062990242
1.837963522	0.393705514	1.838064963	0.787402485	1.83812526	1.062990261
1.871333949	0.39370606	1.871442891	0.787402759	1.871507216	1.062990284
1.904702813	0.393706657	1.904819739	0.787403067	1.904888415	1.062990312
1.938070109	0.393707308	1.938195535	0.787403414	1.938268926	1.062990345
1.971435842	0.393708018	1.971570307	0.787403803	1.97164882	1.062990388
2.00480002	0.393708791	2.004944082	0.787404241	2.005028156	1.062990446
2.038162649	0.393709634	2.03831689	0.787404735	2.038406969	1.062990525
2.071523733	0.393710551	2.071688757	0.787405292	2.071785289	1.06299063
2.10488326	0.393711546	2.105059703	0.787405919	2.105163147	1.062990768
2.138241215	0.393712626	2.138429748	0.787406625	2.138540568	1.062990943
2.171597597	0.393713797	2.171798898	0.787407421	2.17191758	1.062991162
2.204952404	0.393715067	2.205167155	0.787408321	2.205294247	1.062991434
2.238305628	0.393716445	2.238534532	0.787409339	2.238670634	1.062991771
2.271657243	0.393717936	2.271901038	0.787410487	2.272046806	1.062992189
2.305007218	0.39371955	2.305266673	0.787411784	2.305422823	1.062992718
2.33835554	0.393721292	2.338631433	0.78741325	2.338798706	1.06299341
2.371702189	0.393723174	2.371995323	0.787414902	2.372174448	1.062994323
2.405047122	0.393725202	2.40535832	0.787416758	2.405550036	1.062995516
2.438390298	0.393727384	2.438720399	0.787418843	2.438925424	1.062997033
2.471731686	0.39372973	2.472081523	0.787421181	2.472300554	1.062998911
2.505071253	0.393732253	2.505441658	0.787423798	2.505675386	1.063001183
2.538408948	0.393734959	2.538800772	0.787426713	2.539049887	1.063003886
2.571744709	0.393737859	2.572158827	0.787429948	2.572424013	1.063007056
2.605078497	0.393740967	2.605515781	0.78743353	2.605797735	1.063010742
2.638410254	0.393744291	2.638871569	0.787437489	2.639171019	1.063014998
2.671739912	0.393747842	2.672226141	0.787441848	2.672543828	1.063019879
2.705067426	0.393751634	2.705579448	0.787446636	2.705916112	1.06302544
2.738392732	0.393755675	2.738931417	0.787451886	2.739287781	1.063031738
2.771715754	0.393759974	2.772281953	0.787457619	2.772658762	1.063038834
2.805036435	0.393764546	2.805630962	0.787463858	2.806028976	1.06304678
2.838354703	0.393769398	2.838978317	0.787470635	2.839398293	1.063055627
2.871670468	0.393774536	2.872323905	0.787477978	2.872766604	1.063065433
2.904983657	0.393779975	2.905667617	0.787485909	2.9061338	1.063076242
2.938294183	0.393785718	2.939009319	0.787494455	2.93949972	1.063088098
2.97160194	0.393791774	2.972348891	0.787503636	2.9728642	1.063101047
3.004906818	0.393798147	3.005686204	0.787513472	3.006227071	1.06311513
3.038208726	0.393804842	3.039021096	0.787523989	3.039588146	1.063130381
3.071507564	0.393811868	3.072353389	0.787535194	3.072947227	1.063146839
3.104803209	0.393819224	3.105682925	0.787547104	3.106304103	1.06316454
3.138095576	0.39382691	3.13900951	0.787559741	3.139658553	1.063183519

3.171384538	0.393834921
3.204669932	0.393843255
3.237951623	0.393851911
3.271229479	0.393860886
3.30450332	0.393870178
3.337772909	0.393879772
3.371038057	0.39388965
3.404298531	0.393899813
3.437554071	0.393910276

3.172332969	0.787573119
3.205653114	0.787587253
3.238969712	0.787602145
3.272282554	0.787617806
3.305591375	0.787634253
3.338895943	0.787651497
3.372196009	0.787669549
3.405491265	0.787688405
3.438781438	0.787708075
3.472066239	0.78772857
3.505345354	0.787749877
3.538618515	0.787772001
3.571885395	0.787794953
3.605145642	0.78781872
3.638398951	0.787843283
3.671644885	0.787868635
3.704883118	0.78789478
3.738113384	0.787921717
3.771335264	0.787949431
3.804548326	0.787977908
3.837752208	0.788007125
3.87094652	0.788037058
3.904130786	0.788067688
3.937304581	0.788098988
3.970467287	0.788130927
4.003618453	0.788163503
4.036758017	0.78819674

3.173010357	1.063203803
3.206359307	1.063225404
3.239705159	1.063248344
3.273047662	1.063272643
3.306386558	1.063298324
3.339721583	1.063325422
3.373052454	1.063353953
3.406378821	1.063383929
3.439700343	1.063415351
3.473016719	1.063448217
3.506327598	1.06348253
3.539632559	1.063518306
3.572931253	1.06355554
3.606223311	1.063594236
3.639508288	1.063634411
3.67278581	1.063676061
3.706055498	1.063719183
3.739316887	1.063763785
3.772569537	1.063809865
3.805812923	1.063857388
3.839046345	1.063906344
3.8722692	1.063956745
3.905480979	1.064008573
3.938680986	1.064061826
3.971868429	1.0641165
4.005042533	1.064172564
4.038201942	1.064230036
4.071344507	1.06428884
4.104467839	1.064348772
4.137569256	1.064409584
4.170646223	1.064470945
4.203699691	1.06453255

Particle Trajectories In Rig With Different Initial Particle Velocities

Rig Model Initial Velocity= 100ft/s		Rig Model Initial Velocity= 300ft/s		Rig Model Initial Velocity= 500ft/s	
Total Deflection (inches)	0.006666399	Total Deflection (inches)	0.000789867	Total Deflection (inches)	0.000263712
X	Y	X	Y	X	Y
1.634799929	4.866250159	1.754799689	4.866250159	1.874799449	4.866250159
1.694767947	4.866250261	1.934435772	4.866250262	2.17374382	4.866250263
1.754672353	4.866250374	2.11335023	4.866250378	2.470601598	4.866250383
1.814513768	4.866250498	2.291554693	4.866250509	2.765420599	4.866250524
1.874292828	4.866250634	2.469060812	4.86625066	3.058252711	4.866250699
1.934010181	4.866250783	2.645880935	4.866250833	3.349155858	4.866250926
1.993666495	4.866250945	2.822028914	4.866251036	3.638200431	4.86625127
2.053262452	4.866251122	2.997519926	4.866251277	3.925465206	4.866251952
2.112798754	4.866251314	3.172369817	4.866251569	4.211032779	4.866253732
2.172276122	4.866251523	3.346596794	4.866251935	4.494971705	4.8662587
2.231695146	4.866251749	3.520223692	4.86625243	4.777305062	4.866270855
2.29105643	4.866251994	3.693274294	4.86625316	5.057996587	4.866295881
2.35036075	4.866252258	3.86577254	4.866254361	5.336951292	4.866340977
2.409608909	4.866252544	4.037745909	4.866256512	5.614017715	4.866412518
2.468801738	4.866252852	4.209216136	4.866260641	5.888916019	4.86651387
2.527940094	4.866253185	4.380193489	4.866268264		
2.58702487	4.866253545	4.550680421	4.866281681		
2.646056991	4.866253934	4.720671215	4.866304179		
2.705037422	4.866254354	4.890151869	4.866339541		
2.763967168	4.866254809	5.059093338	4.866392068		
2.822847281	4.866255302	5.227448835	4.866466362		
2.881678862	4.866255836	5.395158251	4.866566139		
2.940462793	4.866256414	5.562144845	4.866694295		
2.999200001	4.866257042	5.728300673	4.866853072		
3.057891738	4.866257724	5.893459887	4.867040026		
3.116539329	4.866258468				
3.17514418	4.866259285				
3.233707792	4.866260185				
3.292231768	4.866261183				
3.350717827	4.866262302				
3.409167793	4.866263569				
3.467583538	4.866265027				
3.525966461	4.866266715				
3.584317875	4.866268678				
3.64263952	4.866270982				
3.700933295	4.866273703				
3.759200767	4.866276971				
3.817443616	4.866280965				
3.875664061	4.866285914				
3.933863427	4.866292147				
3.99204239	4.866299962				
4.050202242	4.866309694				
4.108343866	4.866321846				
4.166467322	4.866336985				

4.22457261	4.866355729
4.282660371	4.866378777
4.340731126	4.866406901
4.398784477	4.866440932
4.456819784	4.866481775
4.514836979	4.866530535
4.572835674	4.866588403
4.630814278	4.866656525
4.688770865	4.86673614
4.746702964	4.866828633
4.804608229	4.866935644
4.862484573	4.867058935
4.920328174	4.867199875
4.978134701	4.867359829
5.035900509	4.867540545
5.093621328	4.867743845
5.151290778	4.867971083
5.208900749	4.86822322
5.266444553	4.868501999
5.323914843	4.868808382
5.381300884	4.869142729
5.438592051	4.869507011
5.495775253	4.86990327
5.552833998	4.870331326
5.609747951	4.870790407
5.666488466	4.871280261
5.723029666	4.871800084
5.779341492	4.872346984
5.835374992	4.872916558

Particle Trajectories In Rig With Different Particle Diameters

Rig Model		Rig Model		Rig Model	
Diameter = .005 inches		Diameter = .02 inches		Diameter = .1 inches	
Total Deflection (inches)	0.35944261	Total Deflection (inches)	0.004545871	Total Deflection (inches)	0.057807679
X	Y	X	Y	X	Y
1.742124608	4.866252218	1.742122707	4.866250317	68.58737097	191.584275
1.895980958	4.866256758	1.908123259	4.866250758	75.1228127	191.5842924
2.027184612	4.866262	2.071531407	4.866251259	81.55619149	191.5843121
2.142489214	4.866268038	2.23244997	4.86625183	87.89155532	191.5843345
2.245937286	4.866274972	2.390978404	4.866252481	94.13281976	191.5843602
2.340172435	4.866282901	2.547215747	4.86625323	100.283884	191.5843897
2.427028201	4.866291921	2.701259112	4.866254097	106.3485712	191.5844238
2.507843995	4.866302145	2.853202123	4.866255109	112.3305676	191.5844637
2.583621035	4.866313676	3.003138056	4.866256305	118.2335453	191.5845107
2.655137476	4.866326635	3.151156942	4.86625773	124.0610488	191.5845668
2.723012658	4.866341157	3.29735074	4.866259462	129.8166987	191.584635
2.787737286	4.866357364	3.441819715	4.866261646	135.5044422	191.584721
2.8497158	4.866375397	3.584668999	4.866264609	141.1284185	191.5848376
2.909286448	4.866395417	3.725996526	4.866268833	146.6924832	191.5850039
2.966735867	4.866417615	3.865896144	4.866275162	152.2003312	191.5852531
3.022309934	4.866442214	4.004467616	4.866285069	157.65589	191.5856432
3.076221974	4.86646948	4.141786154	4.866301391	163.0621209	191.5862858
3.128659113	4.866499731	4.277903001	4.866327981	168.4210412	191.5873326
3.179774356	4.866533242	4.412859513	4.866369588	173.734279	191.5889707
3.229703906	4.866570356	4.546675089	4.866432654	179.0025983	191.5914536
3.278583058	4.866611635	4.679343692	4.866523889	184.2257611	191.5950455
3.326521331	4.86665759	4.810830817	4.866651377	189.4024093	191.6000647
3.373618458	4.86670892	4.941097173	4.866824954	194.5309957	191.6068984
3.419965217	4.866766448	5.070082859	4.867055009	199.6091622	191.6159557
3.465643315	4.866831336	5.197690386	4.867350728	204.6330705	191.6275982
3.510726206	4.866904943	5.323796778	4.867718635	209.5978791	191.6420827
3.555277674	4.866988875	5.448245404	4.868164832		
3.599355729	4.867084737	5.570857629	4.868697902		
3.64300364	4.867194845	5.691403044	4.869321119		
3.68627442	4.867320931	5.809507053	4.870027658		
3.729218882	4.867465448	5.924670014	4.870796188		
3.771873591	4.867632017				
3.814272595	4.867823082				
3.856457877	4.868043477				
3.898467264	4.86829882				
3.940323734	4.868593563				
3.982041384	4.868935336				
4.023632103	4.869332674				
4.065099763	4.869791673				
4.106453554	4.870321423				
4.147702596	4.870931092				
4.188848885	4.871626804				
4.229899269	4.872418485				
4.27085967	4.873316427				

4.311734392	4.87433163
4.352526861	4.875475674
4.393238232	4.876761035
4.433868598	4.878200938
4.474412658	4.879803362
4.514852326	4.881580177
4.555180827	4.883545721
4.595401818	4.885711342
4.635502659	4.888092185
4.675469896	4.890703815
4.715286613	4.893562637
4.754917482	4.896682107
4.79434911	4.900072403
4.833566994	4.903751912
4.872531287	4.907734449
4.911194746	4.912034679
4.949532791	4.916673347
4.987520782	4.921660803
5.025096066	4.927011799
5.062191441	4.932740674
5.098776798	4.938858828
5.134818064	4.945377652
5.17022263	4.952314129
5.204936175	4.959691709
5.238937476	4.967521186
5.272167376	4.975809666
5.304553478	4.984565776
5.336016789	4.99379818
5.366536587	5.003524897
5.396072101	5.013766605
5.424523505	5.024542003
5.451812308	5.035872157
5.477947208	5.047782767
5.502927841	5.060301388
5.526651213	5.073452401
5.549135834	5.087270767
5.570405157	5.101798992
5.590513761	5.117081268
5.609600669	5.133134624
5.627681422	5.149980878
5.644870074	5.167663866
5.661416006	5.186199145
5.677498092	5.205564517
5.693247815	5.225694827

Particle Trajectories In Rig With Different Initial Distances from Bleed Wall

Rig Model
Initial Position = .7243 in. from wall

Total Deflection (inches)	0.00012654
X	Y
1.742122549	4.275700159
1.909131204	4.275700309
2.075516331	4.275700575
2.241286748	4.275700975
2.406451427	4.275701538
2.571019311	4.2757023
2.734999496	4.275703299
2.898401867	4.275704591
3.06123646	4.275706251
3.223512994	4.275708376
3.385241277	4.275711101
3.546431322	4.275714613
3.707093512	4.275719169
3.867236304	4.275725121
4.026866811	4.275732937
4.185990003	4.275743245
4.344606981	4.275756799
4.502714403	4.275774488
4.66030507	4.275797417
4.817368914	4.275826699

Rig Model
Initial Position = .3306 in. from wall

Total Deflection (inches)	0.000107792
X	Y
1.742122549	4.590660159
1.909132554	4.59066028
2.075522123	4.590660454
2.241300503	4.59066069
2.406477329	4.590661003
2.571062627	4.590661408
2.735066417	4.590661924
2.898499947	4.590662582
3.061375185	4.59066342
3.223704238	4.590664491
3.385501043	4.590665888
3.546780474	4.590667755
3.707555797	4.590670315
3.867839444	4.590673939
4.027644046	4.590679175
4.186980209	4.590686787
4.345852212	4.590697864
4.504259542	4.59071391
4.662197656	4.590736613
4.819653964	4.590767951
4.976608015	4.590810098
5.133034179	4.590865136
5.288896739	4.590934713
5.444150693	4.591020123
5.598742323	4.591121837

Rig Model
Initial Position = .118 in. from wall

Total Deflection (inches)	0.001049113
X	Y
1.742122549	4.944990159
1.90913225	4.944990258
2.075521003	4.944990361
2.241298304	4.944990468
2.406473674	4.94499058
2.571057726	4.944990699
2.735061754	4.944990825
2.898497289	4.944990961
3.061377876	4.94499111
3.223718654	4.944991276
3.385536142	4.944991467
3.546853118	4.944991713
3.707692587	4.944992107
3.868075721	4.944992796
4.02803055	4.944994274
4.187580411	4.944997576
4.346735717	4.945004102
4.505499311	4.94501594
4.663868814	4.945036314
4.821833313	4.945069046
4.97936809	4.945118465
5.136439035	4.945190059
5.292999625	4.945289041
5.448993542	4.945419229
5.604346078	4.945584701
5.758928816	4.945791439
5.912492465	4.946039272